Available online at www.sciencedirect.com
ScienceDirect
Progress in Materials Science 52 (2007) 540–596
Progress in Materials Science
www.elsevier.com/locate/pmatsci

Roles of minor additions in formation and properties of bulk metallic glasses

Wei Hua Wang *

Institute of Physics, Chinese Academy of Sciences, P.O. Box 603(42-1), Beijing 100080, PR China

Received 15 July 2006; accepted 29 July 2006

Abstract

Bulk metallic glasses (BMGs) are of current interest worldwide in materials science and engineering because of their unique properties. Exploring BMGs materials becomes one of the hottest topics in the materials science field. To date, there is very active worldwide development of new BMGs, and extensive efforts have been carried out to understand and improve the glass-forming ability of metallic materials supported by large government and industry programs in North America, Asia, and Europe. Minor addition or microalloying technique, which has been widely used in other metallurgical fields, plays effective and important roles in formation, crystallization, thermal stability and property improvement of BMGs. This simple approach provides a powerful tool for the BMG-forming alloys development and design. In this paper, we present a comprehensive review of the history and the recent developments of this technique in the field of BMGs. The roles of the minor addition in the formation and the properties of the BMGs and the BMG-based composites will be discussed and summarized within the framework of thermodynamics, kinetics and microstructure. The empirical criteria, or the principles and guidelines for the applications of the technique in BMG field are outlined.

PACS: 61.43.Fs; 62.50.+p; 64.70.Dv; 81.20.n

* Tel.: +86 10 82649198; fax: +86 10 82640223.
E-mail address: whw@aphy.iphy.ac.cn
URL: http://mmp.iphy.ac.cn

0079-6425/$ - see front matter © 2006 Elsevier Ltd. All rights reserved.
doi:10.1016/j.pmatsci.2006.07.003

Contents

1. Introduction

The emergence of bulk metallic glasses (BMGs) with a unique combination of properties has been an important part of the materials science scene over the past decades [1–10]. The new types of metallic glass-forming alloys promise to allow the production of large-scale bulk glassy material by conventional casting processes at low cooling rates.

The BMGs, which exhibit high thermal stability as well as advantageous physical, mechanical and chemical properties, are believed to have considerable application potentials as advanced engineering and functional materials [1–10]. In fact, the Zr-based BMGs have already been applied to industrial fields [11]. Some companies in USA, Japan and China (one of the most famous companies is named Liquidmetal Technologies in USA) have been set up for developing applications of these materials for industries and military purposes [11]. From the glass science point of view, the new atomic metallic glasses with the distinct glass transition and the exceedingly stable supercooled liquid state make it possible to investigate the intrinsic viscous behavior of the supercooled liquid, the relaxation and the glass transition in the metallic alloys with large experimentally accessible time and temperature windows [1–4]. The BMGs are also ideal materials for studying and contrasting some fundamental issues in materials science and condensed matter physics such as deformation and fracture, disorder structure and nucleation. A new class of glassy materials even could have important impact and influence on the scientific community and even daily life [12]. Therefore, the exploration of BMG materials becomes one of the hottest topics in current materials science field. At present, there is very active worldwide development and study of the new BMGs supported by large government and industry programs in North America, Asia, and Europe. The importance of the glassy materials can also be witnessed by a large number of papers on the formation and properties of the materials in archival scientific journals (for overview see Refs. [1–4]).

1.1. The background of the development of bulk metallic glasses

The formation of the first metallic glass of $Au_{75}Si_{25}$ by rapid quenching was reported by Duwez et al. at Caltech, USA in 1960 [13]. They developed the so-called rapid quenching technique for chilling metallic liquids at very high rates of 10^5–10^6 K/s. The significance of Duwez's work was that their method permits large quantities of an alloy to be made into glassy state comparing to that of other methods. Following the studies, the technique of melt quenching had been extensively developed and elaborated for the purpose of producing a wide variety of metallic glasses. The fundamental interest and the properties of technological importance of the metallic glasses were the focus of an explosion of academic and industrial research in that period [14–16]. However, the high cooling rate limits the glassy alloys geometry to thin sheets, powders and lines, which are unlikely to be widely applied in industries. Therefore, a significant aim in this field is to develop new methods to prepare the bulky metallic glasses. Academically, Turnbull and his group had done a critical contribution to the research topic [17–19]. Turnbull et al. had predicted that a ratio of the glass transition temperature T_g to the liquidus temperature T_l of an alloy referred to as the reduced glass transition temperature $T_{rg} = T_g/T_l$, can be used as a criterion to determine the glass-forming ability (GFA) of the alloy [19]. According to the Turnbull's criterion [19], a liquid with $T_{rg} \geqslant 2/3$ should become very sluggish on laboratory time scale and can only crystallize within a very narrow temperature range, and thus can be readily undercooled into the glassy state with a low cooling rate. Up to now, the Turnbull criterion remains one of the best "rule of thumb" for predicting the GFA of any liquid [1–4]. It has played a key role in the development of various metallic glasses including the BMGs.

In 1982, Turnbull et al. [20] successfully found the famous Pd–Ni–P glass-forming alloys by using a boron oxide fluxing method to dissolve heterogeneous nuclei into a glassy surface coating. The fluxing experiment showed that the value of T_{rg} of the Pd–Ni–P alloy

could reach 2/3 when the heterogeneous nucleation was suppressed, and the bulky glass ingot of centimeter size was obtained at a cooling rate of 10 K/s. The Pd–Ni–P is the first bulk metallic glass. In the later 1980s, Inoue group in Tohoko University of Japan succeeded in finding new multicomponent alloys such as La–Al–Ni [21], Mg–Y–Cu [3] and Zr–Al–Ni–Cu [3] consisting mainly of common metallic elements. By casting the melt alloy into water-cooling Cu-molds, fully glassy rods, strips and bars with cast thickness of several millimeters toward several centimeters can be obtained with the low critical cooling rates. Since then, the exploration and studies of the multicomponent BMGs have attracted increasing attention [1–4].

It is apparent that the BMGs are developed in the sequence beginning with the expensive metallic-based Pd, Pt, and Au, and followed by less expensive Zr-, Ti-, Ni- and Ln-based BMGs, and furthermore, it can see that the much cheaper Fe-, Cu- and Mg-based BMGs were the most recently developed [3]. The low-cost metallic-based BMGs had attracted extensive interests because the possibility for a large amount of application as engineering materials.

The internal factors of the alloys (such as the number of the components, purities and the atomic size of the constituent elements, the composition, and cohesion between the metals, etc.) and not the external factors (such as cooling rate, etc.) play a key role in the formation of the BMGs. For designing and developing new BMG-forming alloys, some empirical criteria have been proposed [1–3,22,23], and the known criteria including: (1) multicomponent alloy of three or more elements with a composition close to the deep eutectic; (2) atomic radius mismatch between the components is greater than 12%; and (3) large negative heat of mixing between the main components. A feasible step is to look for the alloy compositions with deep eutectics, which form liquids that are stable to relatively low temperatures [1–3]. One of the general guiding principles to design alloys that form BMGs is to pick multicomponent elements with dramatic differences in size, which leads to an increased complexity and size of the crystal unit cell and reduces the energetic advantage of forming a crystalline intermetallic [22]. The complicated structure with atomic configuration corresponding to a higher degree of dense random packed structure leads to high viscous of the supercooled liquid state and slow crystallization. Along this idea, the minor additions or microalloying method is widely and effectively used to develop the new BMGs, improve the GFA and enhance the properties of the BMG materials [24,25].

1.2. The background of minor addition technique and its applications

The minor addition—the intentional introduction of impurities into a material—is fundamental to controlling the formation, manufacture, and properties of various materials. Because the nucleation of the crystalline phases is relevant for all solidification and the minor addition is an effective way to control the nucleation. From the beginning of our civilization, metalworkers have known that the properties of a metal or alloy can be tailored by minor additions of other elements or materials. For example, in ancient China (about B.C. 3000–1000), the properties of Cu–Sn alloys (bronze) were tailored by proper addition of minor lead. It was known that iron could be hardened or strengthened by proper addition of carbon. The minor addition or microalloying technique was key metallurgical practices and dominant concepts for developing new metallic crystalline materials in the late half of the 20th century [25–27]. However, even though the principles underlying these technologies have been analyzed precisely from theoretical viewpoints,

there remain still some unanswered questions on the actual mechanisms that control the microalloying behavior, which is generally complicated and variable depending on conditions and circumstances. The typical examples of the application of the minor addition technique in metallic materials are briefly described as following:

The first example is the invention of ductile intermetallic Ni_3Al alloys. With addition of 0.1 wt.% boron, the room temperature ductility of Ni_3Al (24 at.% Al) intermetallic was dramatically increased to 53.8% [26,27]. Grain boundary segregation and slowdown of hydrogen diffusion induced by the minor boron addition were responsible mechanisms in this specific crystalline material [26,27].

Pure aluminum is soft and has little strength or resistance to plastic deformation. However, alloyed with small amounts of other elements, it can provide the strength of steel at only half the weight. With thermal treatments, the added alloying elements can form nanometer-sized precipitates, which act as obstacles to dislocations movement in the crystal and strengthen the aluminum. This phenomenon is known as precipitation hardening [28].

This grain refinement brings many benefits in the solidification process itself and in the properties of the as-cast materials. The grain refinement of alloys can be realized by inoculation of melts [28]. The inoculation is the addition of solid particles to a metallic melt to act as nucleant catalysts for the formation of fine equiaxed, rather than columnar grains. In the casting of Al, the most widely used inoculants are those based on AlTiB (notably Al–5wt.%Ti–1wt.%B), AlTiC (Al–3wt.%TiC–0.15wt.%). The AlTiB refiner consists of Al_3Ti and TiB_2 in α-Al matrix. When added to the melt, the matrix melts, the dilution of Ti content leads to rapid dissolution of the Al_3Ti, while TiB_2 remains stable. The TiB_2 particles appear to be coated with a thin layer of Al_3Ti. The nucleant particles are hexagonal platelets of TiB_2-coated with an adsorbed layer of Al_3Ti. Nucleation of α-Al occurs on the faces of the borides with the close-packed planes. While inoculation of Al alloys is aimed at controlling the grain structure, it has additional important effects such as on the selection of secondary intermetallic phases in the alloy [28]. The addition method is of the greatest industrial importance for Al alloys.

Minor addition has been widely used in Mg-based alloys to optimize the properties of the alloys [29]. The minor alloying elements could be from a solid solution together with Al in the matrix of the Mg–Al alloys. They would also form intermetallic phases in the grain boundary zone. Cerium-rich misch metal, for example, has some solid solubility in Mg (at the 0.1 at.% level). The rare earth elements react with Al, forming intermetallic particles, and further reduce the solid solubility. The additions of rare earth elements at a given Al content can improve ductility and castability of the Mg-based alloys.

In steel industry, the minor rare earth material additions have been widely used as a good scavenging flux in the steel melting and casting processes, because the reactions between rare earth elements and harmful impurities are thermodynamically favored compared to that between impurities and Fe. Small amount of rare earth material in the steel melts have the role of scavenging, deoxidization and grain refinement and so on.

The development of minor additions technologies and their responsible mechanisms for crystalline metallic materials in the past is summarized in Table 1. In fact, the minor additions technique is not only applied in metallurgy field, but also widely used in other fields such as the semiconductor industries, the nano-science and technology, and the food industry. For example, for semiconductor devices, precise control of the doping level is also vital.

Table 1
Cases for applying minor additions technique and corresponding mechanisms in metallurgy [24–29]

Period	Technologies	Mechanisms
1920s	Thoria–Tungsten	Surface adsorption
	Grain-oriented Si-steel	Nucleation
1940s	Strengthen Al	Block dislocation movement
	Boron steel	Grain boundary pinning
	Nodular graphite cast iron	Grain boundary segregation
1960s	HSLA steel	Solute drag
1970s	Rare earth element addition in the steels cast	Scavenging the impurities
1980s	Ductile Ni_3Al	Grain boundary segregation and slowdown of hydrogen diffusion
1990s	Refiners Al_5Ti_1B, $Al_3Ti_{0.15}C$	Formation of a fine, uniform, equiaxed grain structure during casting
2000s	Bulk metallic glass-forming alloys	Suppress the completing crystalline phases Stabilize the liquid Scavenging the impurities and oxygen Form BMG-based composites Enhance the properties

1.3. The applications of minor addition technique in BMG field

For the BMG-forming alloys, in which the internal factors such as the number and the nature of the components, the alloy composition as well as the purities is crucial for the glass formation. The GFA and properties of the BMGs are also quite sensitive to the composition. Therefore, the minor addition technique has already played the effective and important roles in glass formation, improvement of thermal stability and properties of BMGs even at the beginning of the birth of BMGs. Table 2 lists the main applications of minor additions in the BMG field.

The addition method is widely applied to explore the new bulk glass-forming alloys. By addition of Cu in PdNiP alloy, the PdNiCuP alloys with the highest GFA so far have been

Table 2
The applications of minor addition in metallic glasses

Functions	Representative references
Enhance the GFA	[2–4,21,24,25,36–40,43,46–51, 66–69,104,108,109]
Explore new BMGs	[1–3,30–40,66–69]
Deteriorate the GFA	[24,25,42–44,52,63]
Scavenging the oxygen in elements and processing environment	[21,23–25,41,42,45–51]
Purify the elements during melting; improve the castability	[21,23–25,44–51]
Induce the formation of BMG-based composites	[52–61]
Enhance the thermal stability	[43,44]
Strengthen the BMG	[36,38,66,67,69]
Enhance the ductility	[66–69,130,175]
Improve the magnetic properties	[62,65,123]
Tune certain physical property	[63–65]

obtained. The critical diameter of the BMG reaches 7–8 cm, and the critical cooling rate of the PdNiCuP alloy is as low as 0.02 K/s [2,30]. A proper addition of Sn in Ti- [31] and Cu-based BMGs [32], and lithium [33] or Ag addition [34] in MgCuY alloys can significantly improve the GFA of these alloys. For the preparation of Fe-based BMG, $Fe_{80}B_{20}$ is often used as the starting alloy, by addition of some metals with high melting temperature, such as Zr, Nb, Ta, W, and Mo, Fe-based BMGs with 5 mm diameters can be obtained by copper mould casting [35]. Very recently, the centimeter-sized BMGs based on ordinary transition metals of Cu [36,37], Fe [38,39] and Mg [40] were developed. The key for the success is attributed to the addition of small amounts of elements such as yttrium, gadolinium into the known glass-forming alloys.

The oxygen and other harmful impurities in the environments and raw materials would dramatically deteriorate the GFA of alloys [2–4]. For Zr-based alloys, high vacuum (at least 10^{-3} Pa), high purity of constituent elements (e.g. the purity of zirconium is at least 99.99 at.%, oxygen content in Zr should be less than 250 ppm) and high purity of argon protecting atmosphere are necessary for the fabrication of the BMGs. Even traces of oxygen or other impurities, e.g., hydrogen, carbon and silicon, would drastically reduce the GFA via the triggering of the heterogeneous nucleation and the formation of nocuous crystalline phases in the undercooled melt [41]. The strict processing condition makes the cost of the BMGs high, and limits its wide applications. Minor addition is effective for improving the processing of the BMGs [24,25,41–51].Minor rare earth addition such as yttrium, gadolinium, or terbium can significantly improve the manufacturability and enhance the GFA of the Zr-, Fe-, Mg- and Cu-based BMG-forming alloys, and the BMGs can be obtained with low purity materials and at a low vacuum condition [41–45]. With proper rare earth element additions the Mg-, and Fe-based BMGs can successfully be fabricated by a conventional Cu-mold casting method even in air atmosphere [46–51].

Minor addition is a promising way for synthesis of novel materials based on BMGs such as nano-materials, glassy matrix composite with the improved mechanical and physical properties [52–61]. The BMG-formers are very robust against some heterogeneous nucleation sites at the surface or at interfaces. This leads to the development of BMG matrix composites by using the addition of elements or special crystalline materials [52–59]. By directly introducing minor dissolution of carbon, carbon fibers, carbon nanotubes, silicon, boron, SiC, WC and ZrC particles into BMGs yields composites. These BMG composites usually have much improved mechanical or physical properties. Minor addition can induced controllable crystallization and form the bulk nanocrystalline or quasicrystalline alloys.

Minor additions can be applied for improving and even tuning the mechanical and physical properties of BMG materials [62–65]. A minor Ni addition can significantly enhance the soft magnetic properties of the Fe-based glass-forming alloys without deteriorating their high GFA. The magnetic and mechanical properties of the rare-earth-based BMGs can be tuned with the varying the of the additional Fe content [63,65]. The addition of the secondary crystalline phases into the metallic glass matrices is an effective technique for improving the ductility of BMGs [2–4,57–59]. By addition of Al into binary $Cu_{50}Zr_{50}$ BMG, the new $Zr_{47.5}Cu_{47.5}Al_5$ BMG exhibits high strength of up to 2265 MPa together with large ductility of 18% [66]. Similar effect of the plasticity enhancement has also been obtained by addition of Ti in CuZr metallic glasses [67], Ta in ZrCuNiAl alloy [68], and Hf (or Zr, Si) in $Ti_{50}Cu_{50}$-based metallic glasses [69].

2. The details of minor addition method

The minor alloying addition method usually follows the following procedure:

(1) The homogeneous ingot of the matrix alloy was prepared by arc melting the mixture of constituent elements in argon atmosphere with high purity.
(2) For the metal or metalloid elements additions, the appropriate amounts of additional element can be directly arc melted with the ingot of the matrix alloy, and the mixture was repeatedly remelted in argon atmosphere to guarantee the homogeneity of the alloy. And then the homogenous melt was sucked or cast directly into a water-cooled copper mold to produce the glassy alloys. To avoid the reaction between the additional element and the components or the matrix, which could trigger the crystallization of the melt and dramatically degrades the GFA of the alloy, the mixture should be melted at a temperature much higher than its melting temperature.
(3) The key step is to obtain homogeneously mixture of the matrix alloy with additional materials especially when larger density and melting temperature difference exists between them. The aggregation of the additional element could dramatically degrade the positive additional effect on the GFA of the alloy.
    (i) For the additional materials that have larger density and melting temperature differences but with a low reactivity with matrix, the key procedure is the homogeneous mixture of the matrix and additional materials and the avoidance the composition precipitation and aggregation. The master ingots and additional materials can be levitating melted and mixed, and then cast into copper mold [47–50].
    (ii) For the additional materials that have large density and melting point differences and high reactivity with matrix. The master ingots and additional materials could firstly be produced in fine powder with the size of about 100–400 μm. The two powders were homogeneously mixed and compressed into a bulky form. The mixed alloy was then quickly remelted and cast into a copper mold [56–60]. The glassy composites synthesized by using addition method sometimes degrade the GFA by altering the composition of the glassy matrices from the optimal composition. Thus, it is important to control the percentage composition of the *in situ* formed second phase. To pinpoint the optimal component needs a long exploring process. The affinity between the additional elements and the BMG–matrix has to be carefully considered. By choosing the right combination of additional material, optimum content and processing, a desired combination of GFA and crystallization can be achieved, and BMG or BMG-based composites can be obtained.

The GFA of the alloys is usually quite sensitive to the fraction of the additional materials, even a minute trace of addition can dramatically enhance the GFA of some alloys; However, the alloying effects of the minor additions on glass formation in multicomponent alloys are often a complex metallurgic phenomenon, and the optimum contents of the additions is normally found to be in a very narrow composition range. Thus, how to pinpoint the optimal fraction of the additional material is important. The selection of the suitable additional materials is important. The guiding principle for the designation and

selection of the suitable additional materials will be described in details in part 8 of this paper.

X-ray diffraction (XRD), chemical composition analysis, differential temperature analysis (DTA), differential scanning calorimeter (DSC), transmission electron microscope (TEM), and high resolution TEM (HRTEM) were applied to study the GFA, composition, microstructure of the alloys. The acoustic measurement, nanoindentation, mechanical test instruments, Physical Property Measurement System were used to studied the physical and mechanical properties of the BMGs with different additions.

3. Improve glass-forming ability by minor additions

In this session, we focus on the effects of minor alloying additions on GFA of BMG-forming alloys. We use the attainable critical thickness (d_c) of fully glassy alloys to indicate the GFA of a BMG-forming alloy. The critical cooling rate required to suppress the formation of a detectable fraction of crystalline phase in quenched fully bulk glassy phase can be roughly estimated by using: dT/dt (K/s) $= 10/(d_c)^2$ (cm) [70]. Other parameters such as the reduced glass transition temperature $T_{rg} = T_g/T_l$ [17–19], the supercooled liquid region ΔT, defined as the temperature interval between the T_g and the onset crystallization temperature T_x [2], and $\gamma = T_x/(T_g + T_l)$ [23] are also used as supplement for evaluating the GFA of the studied alloys.

3.1. The minor additions of metalloid elements

Metalloid elements of Si, C, and B, which could be absorbed easily from the atmosphere and environment during melting, quenching, processing and heat treatment of the alloys, are found to have significantly effects on the GFA, thermal stability, crystallization, and properties of the BMG-forming alloys [24,25,41,43,44,71–74]. These materials have a strong affinity with conventional BMG-forming base elements such as Zr, Ti, Cu, Fe, Mg and rare earth elements, i.e. they have large negative heat of mixing with these base elements [75]. The C, Si, and B can react with the main metallic constituents and form crystalline compounds with a high melting temperature, because the reaction is thermodynamically favored. Therefore, it is expected that the metalloid elements would result in crystallization and degrade the GFA of the BMG-forming alloys. However, on the other hand, due to the small atomic size of the C, B and Si atoms, the proper additions can tighten the alloy structure and then stabilize the alloy against crystallization.

Experimental results indicate that 1–2% carbon addition does not significantly influence the GFA but makes the alloy more thermally stable. For example, the T_x of $Zr_{41}Ti_{14}Cu_{12.5}Ni_{10}Be_{22.5}$ (vit1) is pronouncedly increased by 1–2% carbon addition [43,54,55]. In some Zr-based alloys, additions of carbon at ppm levels with/without small doping of the element B could, to a certain degree, alleviate the detrimental effect of oxygen, thereby improving their GFA [25]. However, even 1 at.% carbon addition results in the formation of crystalline carbide in the ZrAlNiCu BMGs [53]. More than 3 at.% carbon addition induces the formation of the crystalline ZrC carbide in vit1 and other Zr-based BMGs (see Fig. 1) [53–55]. Similarly, more than 1% boron or silicon addition will markedly deteriorate the GFA of the Zr-based BMG-forming alloys [44]. Therefore, in general, the metalloid elements have negative effects on the GFA of the Zr-based alloys, but unlike oxygen (more than 250 ppm oxygen can markedly destroy the GFA of the alloys) [41], the GFA of

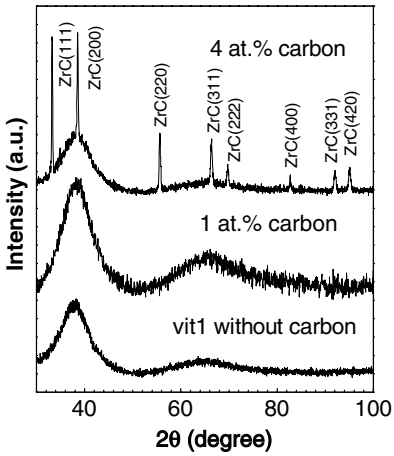

Fig. 1. XRD pattern for the $Zr_{41}Ti_{14}Cu_{12.5}Ni_{10}Be_{22.5}$ alloy with 1 and 4 at.% carbon additions.

the Zr-based alloys are not very sensitive to the metalloid elements, and less than 1 at.% metalloid elements addition usually will not seriously affect their GFA. On the other hand, the reaction between the metalloid elements and base component such as Zr can be utilized to form glassy matrix composites [54].

Silicon is effective in facilitating glass formation for refractory-elements-based and rare-earth-based alloys such as Cu-, Fe-, Ni-, Ti- and Ce-based alloys [76–79]. Only 1% silicon addition in the Cu- and Ti-based alloys can dramatically increases their critical diameter for glass formation [71,76,80]. However, the silicon additions of even 1 at.% are extremely detrimental to the GFA of the Zr-based alloys due to the formation of silicates [54]. Boron additions in Ni-, La-, Fe- and Zr-based BMGs have been found to promote the glass formation [81–85]. For Zr-based alloys, their GFA is extremely sensitive to the boron doping level; additions of less than 0.2 at.% boron, along with other elements like Pb, C, Si, etc., successfully overcome the harmful effect of oxygen [81]. However, when the boron content exceeded 1 at.%, the GFA is thus severely deteriorated by the formation of Zr borides [44].

In the Fe-, Co-, and Ni-based alloys, the proper additional elements like C, B, P or Si play crucial role in the formation of the BMGs. In amorphous steels, the preferable glass-forming composition is approximately formulated as $(Fe_{44.3}Cr_5Co_5Mo_{12.8}Mn_{11.2}C_{15.8}B_{5.9})_{100-x}Y_x$ [38,86,87]. Recently, a cast $Co_{43}Fe_{20}Ta_{5.5}B_{31.5}$ BMG has been designed containing large amounts of boron which exhibits excellent soft magnetic properties, as well as ultrahigh strength over 5000 MPa resulting from the strong bonding nature of Ta–B and Fe–B atomic pairs [86,88]. However, the addition of metalloid elements usually makes the Fe-based BMGs more brittle. The Fe- and Ni-based BMGs so far have very small toughness which approaches the brittle behavior associated with silicate glasses [89–91]. Table 3 summarizes the various effects of metalloid element minor alloying additions in various BMGs-forming alloys.

3.2. The addition of metallic elements

Table 4 lists the different effects of metallic element minor additions in various BMGs-forming alloys. The additions of transitional metals are widely applied in various alloy

Table 3
Summary of the effects of minor metalloid element alloying additions in various bulk metallic glasses

Adding element, *M*	Optimum content *x* (at.%)	Base alloy (at.%)	Effect on glass-forming ability	References
C	<1.0	$Zr_{52.5}Al_{10}Ti_5Cu_{17.9}Ni_{14.6}$	No appreciable difference	[124]
	<2.0	$Zr_{41}Ti_{14}Cu_{12.5}Ni_{10}Be_{22.5}$	Enhance GFA	[43,55]
	<5	FeGaPCB	Enhance GFA	[108]
	<5	Fe-based BMG	Enhance GFA	[45]
	<5	$La_{55}Al_{25}Ni_{20}$	No appreciable difference	[82]
Si	1%	Ti–Zr–Hf–Cu–Ni	Enhance GFA	[71]
	<1.0 at.%	$Zr_{52.5}Al_{10}Ti_5Cu_{17.9}Ni_{14.6}$	No appreciable difference	[124]
	2 at.%	Fe–Ga–P–C–B	Enhance GFA	[108]
	2 at.%	$Ni_{59}Zr_{20}Ti_{16}Si_2Sn_3$	Enhance GFA	[147]
	<5	$Cu_{47}Ti_{34}Zr_{11}Ni_8$	Enhance GFA	[76]
	<5	Ni–Ti–Zr–Si	Enhance GFA	[77]
	<5	Fe–Al–Ga–P–C–B–Si	Enhance GFA	[78]
B	1–10%	$Fe_{91-x}Zr_5B_xNb_4$	Enhance GFA	[74]
	<5	FeGaPCB	Enhance GFA	[108]
	<5	Fe-based BMG	Enhance GFA	[45]
	<5	$La_{55}Al_{25}Ni_{20}$	No appreciable difference	[82]
	2	Ni–Nb–Sn	Enhance GFA	[83]
		ZrCuAl	No appreciable difference	[85]

systems to develop new BMGs, and to improve the GFA and properties of the BMG-forming alloys.

Larger metallic atoms, such as Zr and Sn are helpful in terms of glass formation [76,83,92]. The addition of Zr in Co-based alloys can significantly enhance the GFA, and the obtained $Co_{40}Fe_{22}Nb_{8-x}Zr_xB_{30}$ ($x = 0$–8) BMGs have a high stability of supercooled liquid and good soft magnetic properties [92]. Replacing only 2 at.% of Ni with Sn in alloy $Cu_{47}Ti_{33}Zr_{11}Ni_8Si_1$ increases its maximum size for glass formation by 2 mm [76]. The large rare earth elements, such as Y, Sc, Gd, Er, etc., even in minute addition have been shown to be beneficial in bulk glass formation. This effect will be specially emphasized in the next section. However, it is to be noticed that the larger metallic atoms such as Hf, Zr, Sn, Mg have negative effects on the GFA of the rare-earth-based BMGs, such as Ce-based BMGs [79]. Some large elements like Ca and Sb also have negative effects on the GFA of Zr- and Ti-based BMGs [24,25].

The intermediate transitional metallic atoms of Fe, Ni, Co, Cu, Mo, Zn, Nb, Ta and Ti have been widely selected as minor alloying elements in various alloy systems. However, only when their alloying quantities exceed 5 at.% have they been shown to be beneficial in bulk glass formation [93–102]. For example, in order to improve the GFA of $Mg_{65}Cu_{25}Y_{10}$ alloy, the addition of Zn has to be at least 5 at.% [96]. In (Ti,Zr)–(Cu,Ni) pseudobinary system, the GFA is significantly improved by the addition of more than 3 at.% Ni into the Ti–Cu binary alloys [101]. The addition of more than 5 at.% Co or Ni element causes an increase of the GFA of $Cu_{60}Zr_{30}Ti_{10}$ alloys [94]. The bulk glassy $(Cu_{0.6}Hf_{0.25}Ti_{0.15})_{98}M_2$ (M = Mo, Ta and Nb) alloys with high thermal stability were synthesized by the additions of elements Mo, Ta and Nb. The maximum diameter for glass formation of 2 at.% Mo, 2 at.% Ta and 2 at.% Nb alloys was 1.5 mm, 3.5 mm and

Table 4
Summary of the effects of minor metallic element alloying additions in various bulk metallic glasses

Alloying element, M	Optimum content x (at.%)	Base alloy (at.%)	Effect on glass-forming ability	References
Fe	2%	$Zr_{41}Ti_{14}Cu_{12.5}Ni_{10-x}M_xBe_{22.5}$	No appreciable difference	[93]
	1%	$(Cu_{60}Zr_{30}Ti_{10})_{100-x}M_x$	Deteriorated	[94]
	1–2%	$Ce_{70-x}Al_{10}Cu_{20}M_x$	Enhanced	[105]
	1–5%	$(Nd_{60}Al_{10}Ni_{10}Cu_{20})_{100-x}M_x$	Deteriorated	[63]
	1–5%	$(Pr_{60}Al_{10}Ni_{10}Cu_{20})_{100-x}M_x$	Deteriorated	[65]
	1–5%	$(Cu_{50}Zr_{50})_{100-x}M_x$	Deteriorated	[102]
Ni	1–3%	$(Cu_{60}Zr_{30}Ti_{10})_{100-x}M_x$	Deteriorated	[94]
	1%	$Ce_{70-x}Al_{10}Cu_{20}M_x$	Enhanced	[105]
	3%	$Ti_{40}Zr_{25}Ni_3Cu_{12}Be_{20}$	Enhanced	[106]
Al	1–5%	$(Cu_{50}Zr_{50})_{100-x}M_x$	Enhanced	[102]
	1–2%	$Fe_{61}Co_7Zr_{10}Mo_5W_2M_x$	Enhanced	[62]
	<10%	$Gd_{60-x}Cu_{20}Ni_{20}M_x$	Enhanced	[113]
Co	1%	$(Cu_{60}Zr_{30}Ti_{10})_{100-x}M_x$	Deteriorated	[94]
	~1%	$Ce_{70-x}Al_{10}Cu_{20}M_x$	Enhanced	[105]
Cu	2.5%	$Nd_{60-x}Fe_{20}Al_{10}Co_{10}M_x$	Deteriorated	[95]
	1%	$Ce_{70-x}Al_{10}Co_{20}M_x$	Enhanced	[105]
Mo	2%	$(Cu_{60}Hf_{25}Ti_{15})_{100-x}M_x$	Deteriorated	[97]
	2–4%	$(Fe_{0.7}Mn_{0.3})_{65}Zr_4Nb_4M_xB_{24}$	Enhanced	[86]
	0.5%	$(Cu_{47}Zr_{11}Ti_{34}Ni_8)_{99.5}M_{0.5}$	No appreciable difference	[76]
	<3%	$(Cu_{0.64}Zr_{0.36})_{1-x}M_x$	Enhanced	[107]
	2 at.%	Fe–Ga–P–C–B	Enhance GFA	[108]
Zn	5%	$Mg_{65}Cu_{25-x}Y_{10}M_x$	Enhanced	[96]
	5%	$Ce_{70-x}Al_{10}Co_{20}M_x$	No appreciable difference	[65]
Nb	1%	$Ce_{70-x}Al_{10}Cu_{20}M_x$	Enhanced	[105]
	1–5%	$Zr_{41}Ti_{14}Cu_{12.5}Ni_{10-x}M_xBe_{22.5}$	No appreciable difference	[103]
	2.5%	$(Zr_{65}Al_{10}Cu_{15}Ni_{10})_{100-x}M_x$	Enhanced	[98,61,137]
	2%	$Fe_{72-x}Al_5Ga_2P_{11}C_6B_4M_x$	Deteriorated	[99]
	4%	$(Co_{70.5}Fe_{4.5}Si_{10}B_{15})_{100-x}M_x$	Enhanced	[100]
	2–4%	$(Fe_{0.7}Mn_{0.3})_{65}Zr_4Nb_4M_xB_{24}$	Enhanced	[86]

(*continued on next page*)

Table 4 (*continued*)

Alloying element, M	Optimum content x (at.%)	Base alloy (at.%)	Effect on glass-forming ability	References
	2%	$(Cu_{60}Hf_{25}Ti_{15})_{100-x}M_x$	No appreciable difference	[97]
	<3%	$(Cu_{0.64}Zr_{0.36})_{1-x}M_x$	Enhanced	[107]
Ta	2%	$(Cu_{60}Hf_{25}Ti_{15})_{100-x}M_x$	Deteriorated	[97]
	2%	$Zr_{41}Ti_{14}Cu_{12.5}Ni_{10-x}M_xBe_{22.5}$	No appreciable difference	[24]
	<5%	$Ni_{60}Nb_{40-x}Ta_x$	Enhanced	[65]
	<3%	$(Cu_{0.64}Zr_{0.36})_{1-x}M_x$	Enhanced	[107]
Ti	1%	$Zr_{60}Cu_{20}Ni_{10-x}Al_{10}M_x$	Deteriorated	[110]
	5%		Enhanced	[110]
	1–5%	$(Cu_{50}Zr_{50})_{100-x}M_x$	Enhanced	[83]
	1–5%	$Zr_{56.2-x}Ti_xCu_{31.3}Ni_{4.0}Al_{8.5}$	Enhanced	[104]
Zr	2%	$Co_{40}Fe_{22}Nb_{8-x}B_{30}M_x$	Enhanced	[92]
	2%	$(Y_{56}Al_{24}Co_{20})M$	Enhanced	[115]
	<3	$Ce_{70-x}Al_{10}Cu_{20}M_x$	No appreciable difference	[65]
Sn	3%	$Ni_{60}Nb_{40-x}M_x$	Enhanced	[83]
	<3	Ti-based BMGs	Enhanced	[31]
	1%	$(Cu_{60}Zr_{30}Ti_{10})_{100-x}M_x$	Enhanced	[76]
	2%	$Cu_{47}Ti_{33}Zr_{11}Ni_{8-x}Si_1M_x$	Enhanced	[76]
	<3%	$(Cu_{0.64}Zr_{0.36})_{1-x}M_x$	Enhanced	[107]
	<8	$(Cu_{40}Ti_{30}Ni_{15}Zr_{10})_{100-x}Sn_x$	Enhanced	[32]

Ag	8.5	$Mg_{54}Cu_{26.5}Ag_{8.5}Gd_{11}$	Enhanced	[40]
	<3%	$(Cu_{0.64}Zr_{0.36})_{1-x}M_x$	Enhanced	[107]
	<5	MgCuY	Enhanced	[34]
Cr, W	0.5%	$(Cu_{47}Zr_{11}Ti_{34}Ni_8)_{99.5}M_{0.5}$	No appreciable difference	[76]
	<3	$Ce_{70-x}Al_{10}Cu_{20}M_x$	No appreciable difference	[105]
Y	2	FeCoCrMoCBY	Enhanced	[39]
	5	ZrTiCuNi	Enhanced	[42]
	<5	Fe-based BMG	Enhanced	[87]
	<15	Mg–Cu-based BMG	Enhanced	[112]
	<3	CuZrAl	Enhanced	[36]
Gd	<15	Mg–Cu-based BMG	Enhanced	[49]
	<5	CuZr-based BMG	Enhanced	[37]
Sc	<0.1 at.%	$Zr_{52.5}Al_{10}Ti_5Cu_{17.9}Ni_{14.6}$	Markedly enhanced	[124]
	<15	Mg–Cu-based BMG	Enhanced	[112]
	<1	$Zr_{55}Al_{10}Cu_{30}Ni_5$	Enhanced	[138]
Er	<5	$Co_{60}Cr_{15}Mo_{14}C_{15}B_5$	Enhanced	[126]
	<15	Mg–Cu-based BMG	Enhanced	[49]
	<2	FeMoCBEr	No appreciable difference	[175]

4.0 mm, respectively [97]. In CuZr binary alloys, when more than 4% Al or Ti or Ta is added, the GFA of the alloy is dramatically increased and the full amorphous rod can be produced up to 5 mm at least [102]. More than 5% addition of Fe, Ti and Nb can improve the GFA of the ZrAlNiCu alloys [93,103,104]. Ma et al. [104] found that a significant increase in the GFA of more than 100% in terms of the diameter of the glass formed from the $Zr_{56.2}Cu_{31.3}Ni_{4.0}Al_{8.5}$ alloy with the addition of 4.9% Ti. They use a computational thermodynamic strategy to obtain a minor but optimum amount of additional Ti element into a base alloy to improve its GFA.

For rare earth-, Ti- and Cu-based BMGs, these intermediate metallic atoms are found to have dramatic effects on GFA with minor additions (<2 at.%) [79,105–107]. Ni addition of no more than 3 at.% is quite critical for the suppression of quasicrystalline phase formation upon solidification in $Ti_{40}Zr_{25}Ni_3Cu_{12}Be_{20}$ BMG which has significant plasticity [106]. A series of Cu–Zr-based bulk metallic glasses $(Cu_{64}Zr_{36})_{1-x}M_x$ are discovered with minor Nb, Sn, Mo, Ag, and Ta additions (lower than 3 at.%) [107]. The minor addition of small amounts of Si and Mo (~2 at.%) is effective for the suppression of precipitation of $(Fe,Mo)_{23}(B,C)_6$ phase in soft magnetic FeMoGaPCBSi BMG-forming alloy, resulting in the extension of the supercooled liquid region, the improvement of GFA and enhanced magnetic properties [108]. In Ce-based BMGs, it is found that even a minute of addition of the intermediate atoms such as Co, Nb, Fe, etc. (<1%) have the most efficient effect on the GFA of the matrix Ce–Al–Cu [79]. The critical diameter of the fully glassy Ce–Al–Cu–X (X represents additional elements) alloys is drastically enhanced from 2 mm (for CeAlCu BMG) to 5–10 mm. For Co addition, even with 0.2 at.% addition can greatly improve GFA of the CeAlCu alloy, and increase its critical diameter from 2 to 8 mm [109].

The beryllium has the smallest atomic size among the metallic elements. The minor Be addition could be very effective in improving the GFA and properties of the alloys. Be content in ZrTiCuNi alloys greatly improves the GFA of the alloys, and the vit alloy system (ZrTiCuNiBe BMGs) is one of the best BMG-forming alloys [2]. Because the element is deadly harmful to the human health, little work has been done on the minor Be alloying addition on various BMG-forming systems.

3.3. The minor additions of rare earth elements

As ''the vitamin of modern industry'', rare earth (RE) elements are the important minor addition materials which have a unique and important impact on the modern industries such as special glass production and metallurgical manufacturing [111]. In the BMG field, the rare earth elements, even in the initial stage of the BMG development in 1990s, have been used as both the good BMG-forming base (e.g. La-, and Nd-based BMGs) and the minor alloying additions [2–4]. Now, it is found that the most RE elements are both the good BMG-forming base [2–4,112–120] and the effective minor alloying elements [24,25,36,38–40,42,45–51,121–125]. Since the RE elements and related RE crystalline compounds have plentiful and unique physical properties, and usually used as functional materials [111], the RE-based or RE additional BMGs could be of potential for application as functional materials.

Yttrium is one of the magic minor addition elements for improving GFA and manufacture of the BMG-forming alloys [24,25,42]. Fig. 2 shows XRD patterns of $(Zr_{55}Al_{15}Ni_{10}Cu_{20})_{100-x}Y_x$ ($x = 0$, 0.5, 1, 2, 4, 6 at.%) alloys (all the samples is in rod shape with a diameter of 5 mm). The as-cast $Zr_{55}Al_{15}Ni_{10}Cu_{20}$ alloy with the low purity of the compo-

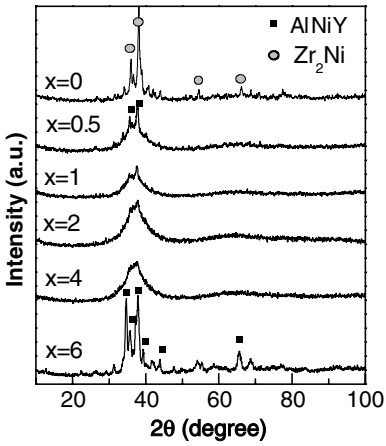

Fig. 2. XRD patterns of the $Zr_{55}Al_{15}Ni_{10}Cu_{20}$ alloy prepared by using low purity of Zr, and the $(Zr_{55}Al_{15}Ni_{10}Cu_{20})_{100-x}Y_x$ (Y = 0.5–6 at.%) alloys with different Y additions.

nents (The purity of Zr, Ni, Cu is less than 99.5%) contains a cubic Zr_2Ni Laves phase. The 0.5 at.% yttrium addition suppresses the precipitation of the Zr_2Ni Laves phase, but another AlNiY crystalline phase is induced in the glassy matrix. With the increase of Y addition from 1% to 2%, the crystalline AlNiY peaks become fewer and weaker. When the yttrium addition reaches 4%, almost no crystalline diffraction peaks are observed, and fully glass is formed within the limit of the XRD detection. Further addition of Y ($\geqslant$6%) also leads to the precipitation of crystalline AlNiY. The result confirms that a proper yttrium addition ($1 < Y < 6$ at.%) can greatly improve the GFA of the Zr-based alloy by suppressing the precipitation of the Zr_2Ni Laves phase.

Fig. 3 presents the DTA curves of $(Zr_{55}Al_{15}Ni_{10}Cu_{20})_{100-x}Y_x$ alloys with a heating rate of 0.33 K/s. No exothermic peak is observed for the alloy without yttrium addition, meaning almost no amorphous phase formed in the as-cast $Zr_{55}Al_{15}Ni_{10}Cu_{20}$ alloy consisting of

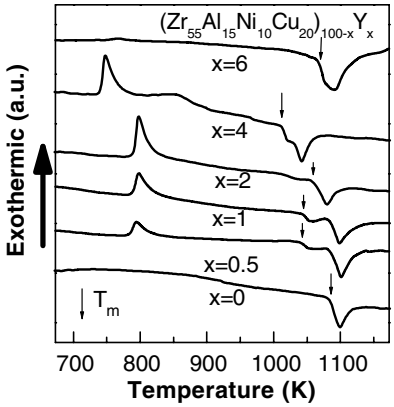

Fig. 3. DTA traces of the $(Zr_{55}Al_{15}Ni_{10}Cu_{20})_{100-x}Y_x$ alloys with a heating rate of 0.33 K/s. T_m is the melting temperature.

low purity components. With 0.5 at.% yttrium addition, an exothermic peak is observed, confirming the formation of amorphous phase induced by minor yttrium addition. For the alloys with 2–4 at.% yttrium addition, the DTA traces exhibit distinct exothermic peaks confirming that the large fraction of amorphous phase was formed in these alloys. With 6 at.% yttrium addition, there is no exothermic reaction occurring, indicating no amorphous phase formed in the alloy. The results are in a good agreement with the XRD results, which indicate that a small and proper amount of yttrium addition can suppress Laves phase formation and greatly increase the GFA of the $Zr_{55}Al_{15}Ni_{10}Cu_{20}$ alloy. DSC curves also show that the yttrium addition clearly decreases the melting temperature of the alloy. Yttrium has also been introduced in the ZrTiCuNiBe and other glass-forming alloys with low purity of the components, fully amorphous alloy with nomination composition of $(Zr_{41}Ti_{14}Cu_{12.5}Ni_{10}Be_{22.5})_{98}Y_2$ is obtained. Previous works indicate that a small amount of yttrium addition can effectively modify the GFA and the crystallization process of a variety of Zr-based alloys [24,25].

Yttrium addition can improve the GFA of Cu- and Fe-based BMGs as well [36,38,45,86,87,102,125]. A minor addition of yttrium (1–2%) can markedly improve the manufacturability of $Cu_{48}Z_{48}Al_4$ alloy via the suppression of the growth of eutectic clusters and the precipitation of the primary dendrite phase [125]. Microalloying with 2 at.% yttrium in Fe-based alloys greatly enlarged their attainable maximum sizes for these alloys even with low-purity raw materials [38,45,86,87]. Also, yttrium is found to be able to not only scavenge oxygen from the undercooled liquid but also lower the liquidus temperature in Fe-based alloys [38,62,86,87]. It is interesting to note that yttrium itself is an excellent BMG-forming base. A family of yttrium metallic alloys is able to form glassy ingots directly from the liquid, or to form bulk-sized glassy rods with a diameters over 2 cm by water quenching of the alloy melt sealed in quartz tubes [115].

The RE elements have similar atomic size, chemical and physical properties. In principle, through the proper addition, other RE elements should have the similar beneficial effect on the GFA of the BMG-forming alloys. In fact, the similar beneficial effect of Sc, La was observed in Zr-based alloys [124]. With the additions of 300–600 ppm Sc, the maximum diameter for glass formation of $Zr_{52.5}Al_{10}Ti_5Cu_{17.9}Ni_{14.6}$ (containing 90–120 wppm oxygen) was increased from 4.5 to 12 mm. Other rare earth elements erbium, dysprosium, holmium, gadolinium have the similar effects on the GFA of the Fe-, Ni-, and Co-based alloys even in minor content [47,126]. The critical diameter of the CoCrMoCB glassy rods can be increased from 2 mm to 10 mm by 2 at.% Er addition. The minor Er addition successfully suppresses the precipitation of the crystalline Co_6Mo_6C phase in the undercooled liquid on cooling [126].

It is known that the manufacturability and the GFA of the BMG-forming alloys are sensitive to the preparation and processing conditions such as vacuum and impurity of environment, because oxygen and other harmful impurities in the environments would significantly deteriorate the GFA. RE elements are found to have magic effect on the manufacturability of some BMGs [47–51]. A variety of RE elements minor additions are able to significantly improve the GFA and withstand a low vacuum in preparation process of Mg-based alloys. A series of ternary Mg–Cu–RE alloys with exceptional GFA and high oxygen resistance during preparation process are successfully prepared by the conventional Cu-mold casting [47–51]. Although further work is necessary to clarify the mechanism for the high oxidation resistance induced by the RE element addition, it is clearer that the Mg-based BMG-forming alloys with RE content are inert in the oxygen and have very

high oxidation resistance and good manufacturability. Fig. 4 presents the XRD patterns of a Tb-bearing $Mg_{65}Cu_{25}Tb_{10}$ BMG (or MgCuPr BMG) (up to 5 mm diameter) synthesized by a normal casting method in air and argon conditions. The results indicate that the alloy cast both in Ar and air conditions contains mainly amorphous phase. Fig. 5 shows the DSC traces of the as-cast $Mg_{65}Cu_{25}Tb_{10}$ alloy prepared in argon and air atmospheres. Comparison of the values of T_{rg}, and crystallization enthalpy ΔH_x for the two alloys confirms that the preparation of the alloy in air condition does not markedly deteriorate its high GFA as other BMG-forming alloys do. Fig. 6 is the photos of the surfaces of $Mg_{72}Cu_{28}$ (Fig. 6(a)) and $Mg_{65}Cu_{25}Tb_{10}$ master alloys (Fig. 6(b)). The $Mg_{65}Cu_{25}Tb_{10}$ alloy shows smooth appearance morphology after melting, and its oxide film is quite different from that of the $Mg_{72}Cu_{28}$ alloy, which burns up during melting and shows the dark products similar to "cauliflower" morphology. The composition analysis shows that the surface region has much high oxygen content compared to that in the center region. The composition of the master alloy is close to the nominal composition of $Mg_{65}Cu_{25}Tb_{10}$,

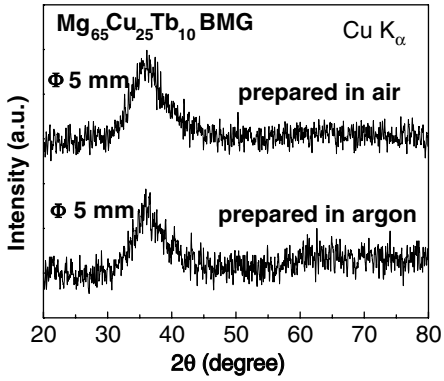

Fig. 4. XRD patterns of the $Mg_{65}Cu_{25}Tb_{10}$ alloy prepared by Cu mold casting in air and argon atmosphere [51].

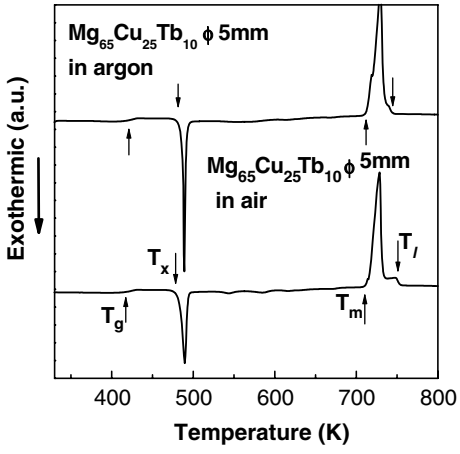

Fig. 5. DSC traces of the $Mg_{65}Cu_{25}Tb_{10}$ BMG prepared in air and argon atmosphere [51].

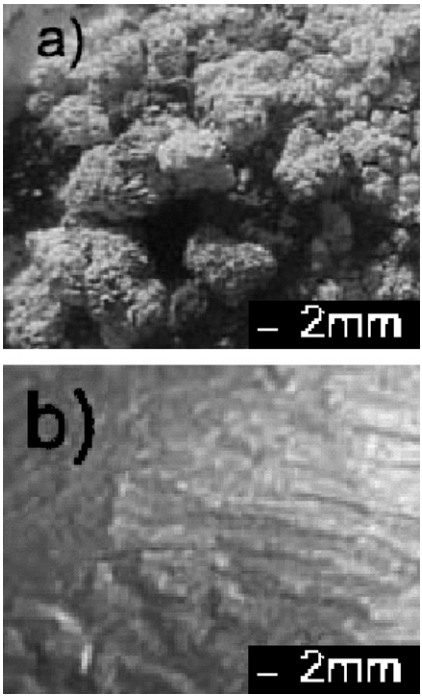

Fig. 6. The photos of master alloy surfaces of the $Mg_{72}Cu_{28}$ (a), and the $Mg_{65}Cu_{25}Tb_{10}$ (b) [51].

and the oxygen content is only about 0.1–0.2 at.%. These results suggest that the formed Tb oxide film plays a crucial role in the particularly high ignition and oxygen resistances of this alloy. The above results demonstrate that the GFA and manufacturability of the $Mg_{65}Cu_{25}Tb_{10}$ alloy are much improved with the addition of Tb. Other RE element additions and even the Tb-rich Misch rare earth are also effective to improve the GFA and manufacturability of the Mg–Cu alloy as well [122]. In fact, other RE-bearing BMGs (e.g. the Zr-, Cu-, Fe-based BMGs) or polycrystalline materials can also be manufactured in air atmosphere. The RE additions provide a feasible approach for improving the manufacturability of BMGs [122].

3.4. The poisons for GFA of alloys

Some additional elements can be a poison for the GFA and properties of BMG-forming alloys as well [41,127–136]. Minor additions or absorptions, even in minute trace, can act as nucleant catalysts for the formation crystalline phase such as Laves phases which can trigger avalanche-like crystallization of the supercooled liquid, and then dramatically deteriorate the GFA and even weaken the properties of the alloys. Oxygen in environment or as impurity in component has significant negative effect on GFA of a variety of BMG-forming alloys [25,41,127–129]. Fig. 7 shows the oxygen effect on the formation of Zr-based BMG. The ZrAlNiCu alloys have excellent GFA (the critical diameter of the BMG rod can reach ~10 mm) when they are prepared at high vacuum condition using components with high purity [3]. However, the XRD patterns of the $Zr_{55}Al_{15}Ni_{10}Cu_{20}$

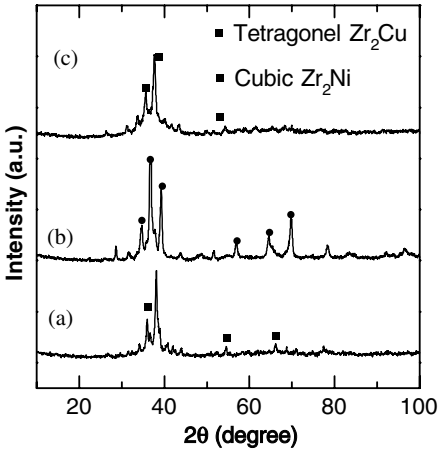

Fig. 7. XRD patterns of $Zr_{55}Al_{15}Ni_{10}Cu_{20}$ alloy (a), and $Zr_{65}Al_{7.5}Ni_{10}Cu_{17.5}$ alloy (b) prepared by using low purity of Zr at low vacuum, and $Zr_{55}Al_{15}Ni_{10}Cu_{20}$ alloy (c) by using the high purity of Zr at a low vacuum.

(Fig. 7(a)) and $Zr_{65}Al_{7.5}Ni_{10}Cu_{17.5}$ (Fig. 7(b)) alloys prepared using a low purity of zirconium (99.8% including 1500 ppm oxygen) at a low vacuum ($\sim 10^{-1}$ Pa) show that crystalline compound precipitates and almost no amorphous phase is formed in the alloy. The $Zr_{55}Al_{15}Ni_{10}Cu_{20}$ alloy (Fig. 7(c)) with high purity of Zr (99.99 at.%) at the same vacuum condition shows a diffused peak superimposed by some crystalline peaks. The main precipitation phase is tetragonal Zr_2Cu ($MoSi_2$ type, space group of $I4/mmm$) in the $Zr_{65}Al_{7.5}Ni_{10}Cu_{17.5}$ alloy, while cubic Zr_2Ni (Al_2Cu type, space group $Fd\bar{3}m$) is the main precipitation crystalline phase in the $Zr_{55}Al_{15}Ni_{10}Cu_{20}$ alloy. The XRD results clearly indicate the dramatic negative effect of oxygen on the GFA of the typical Zr-based BMG-forming alloys. Altounian et al. [129] also found that oxygen can greatly enhance and stabilize the formation of cubic Zr_2Ni phase in binary Zr–Ni alloy. Eckert et al. [128] found that oxygen induced cubic phases (such as Zr_2Ni.) in the $Zr_{65}Al_{7.5}Ni_{10}Cu_{17.5}$ alloy. Gebert et al. [41] verified that oxygen triggered nucleation of cubic Zr_2Ni phase which acted as heterogeneous nucleation sites for crystallization of other stable phases such as tetragonal Zr_2Cu in the $Zr_{65}Al_{7.5}Ni_{10}Cu_{17.5}$ alloy. Conner et al. [57] found that oxygen addition accompanies by the formation of Zr_2Cu- and Zr_2Ni-type intermetallic oxide particles in ZrNbAlCuNi BMG. The formation of crystals results in the complete loss of compressive and bending ductility. Combining with above results, it is conclude that the crystalline precipitation in the Zr-based alloys results from oxygen contamination introduced both from the raw materials and the low vacuum. Similar results have been found in the systems of Fe-, Cu-, Ti-based BMG-forming alloys. In commercial applications, one of the greatest setbacks of this oxygen sensitivity is the high cost of raw materials with low oxygen impurity levels.

Oxygen effects on crystallization in Zr-based alloys have also been well studied [41,127,128,133]. The high oxygen content induces the precipitation of metastable quasicrystalline phases in these alloys and, in turn, significantly destabilize the supercooled liquid, i.e. drastically decreases the value of the supercooled liquid temperature region ΔT. The metastable phases with oxygen up to 4 at.% are detected in a nanocrystallized Zr-based metallic glass. The influence of oxygen on the kinetics of crystallization is attributed to the formation of the oxygen enriched metastable phases during annealing [134,135].

There is little work on the effect of hydrogen on GFA of the BMG-forming alloy. Huett et al. [131] found that the hydrogenation concentration moved the glassy $Zr_{69.5}Cu_{12}Ni_{11}Al_{7.5}$ material out of its stability range, and the hydrogen in the glassy alloy also changed the phase evolution. The variations in the structure, thermal and mechanical properties of $Zr_{50}Ni_{27}Nb_{18}Co_5$ BMG, upon electrochemical charging with hydrogen were investigated by Jayalakshmi et al. [136]. Structural analysis shows that the amorphous nature of the alloy is retained for low hydrogen concentrations. But beyond a critical concentration, hydrogenation of the glassy alloy plays a major role in altering the structural and thermal stability, and mechanical properties. Particularly, for relatively high concentrations (>16 at.%), hydrogen induced nanocrystallization and simultaneous reduction in fracture strength were observed. Hydrogen embrittlement occurred at high concentrations is attributed to the reduction in cohesion between atoms due to the presence of hydrogen. Kokanovic and Tonejc [132] found that adding hydrogen to the partially crystalline $Zr_{76}Ni_{24}$ metallic glass raised the temperature of crystallization in the composite on range of hydrogen content lower than $x \leqslant 0.05$ at.%.

The metalloid elements Si, C, and B have a stronger affinity with BMG-forming base elements such as Zr, Ti, Cu, Fe, Mg and rare earth elements. These additional elements are thermodynamically favored to react with the main metallic constituents and form the crystalline compounds, which trigger the crystallization and deteriorate the GFA of the alloys. Carbon, silicon can be absorbed easily from the atmosphere and environment during melting, quenching, processing and heat treatment of the alloys. Therefore, clean environment are necessary for BMGs processing especially for Zr-, Cu- and Ti-based BMG-forming alloys.

4. The BMG–matrix composites formed by additions

The BMG materials have unique properties which lead to outstanding application potentials instead of traditional crystalline metals [1–4]. However, the BMG materials also have some intrinsic flaws which restrict their applications. For example, the ductility of BMGs at room temperature is usually disappointedly low due to the lack of dislocation systems and grain structure [139–141]. Upon yielding, the plastic deformation of the BMGs is highly localized into shear bands. These shear bands can rapidly propagate across the sample after their initiation, and initiate cracking and lead to limited global ductility (less than 1%) and macroscopic catastrophic fracture. This restricts the use of BMGs as the engineering material [1–4]. In an effort to overcome the intrinsic problems of BMGs, recently, there have been considerable scientific and industrial interests in a variety of BMG composites as a way to further improve mechanical properties compared to monolithic BMGs [57–59,66,142,143]. A variety of BMG composites have been made by adding the second crystalline phase in the BMG-forming melts or by *in situ* formation of crystalline phase through partial crystallization in the glassy matrix [57–59,66,142,143]. The ultimate aim of this approach is to restrict the rapid propagation of the shear bands by interaction with the ductile crystalline phases. BMGs themselves are also interesting matrix materials for composites because of their low melting points (normally <1000 K) and their high resistance against heterogeneous nucleation of crystals. The BMG–matrix composites formed by minor additions do have much improved mechanical and physical properties.

4.1. The BMG–matrix composites with enhanced strength

The reinforcements such as particulate diamonds, filamentary SiC, TiC, WC, tungsten metal particles, tungsten wires, ceramic particles can be directly introduced into the BMGs. The formed composites have much enhanced strength [1,2]. Since carbon can form strong covalent bonds with Zr and Ti constituents in the Zr-based alloys and cause the formation of carbide crystalline compounds with high strength, the BMG–matrix composites can be *in situ* obtained by minor additions of carbon [54]. More than 3 at.% carbon addition induces the formation of crystalline ZrC carbide on the amorphous matrix in $Zr_{41}Ti_{14}Cu_{12.5}Ni_{10}Be_{22.5}$ (see Fig. 1). The fabrication of the glass-based composite containing the homogeneously ceramic fcc-ZrC particles is up to 8% carbon addition [54]. The uniformly dispersed ZrC particles increase effectively the mechanical properties of the BMG–matrix composites, since the Young's modulus E and Vickers hardness (H_v) of the ZrC carbide have been reported to be 390 GPa and 32 GPa, respectively. Fig. 8 shows the influence of carbon addition on the H_v of the alloy. The H_v increases with increasing carbon content. The elastic behavior studied by ultrasonic technique shows that the E changes from 90 GPa for the homogenous vit1 to 106 GPa for the BMG with 1% carbon addition confirming that little carbon addition can enhance the strength of the BMG [144]. The similar tendency is also found for ZrAlNiCu composite containing ZrC particle [53]. The *in situ* formed Mg-based BMG composites consisting of uniformly distributed Fe-rich particles of 1–10 mm in size show a fracture strength as high as 990 MPa and a plastic strain of about 1.0% before failure in uniaxial compression [145]. The Fe addition has no adverse effect on the GFA of the Mg-based matrix and delays the catastrophic failure of the BMG, leading to observable yielding and a high compressive strength. Fe has a positive heat of mixing with the majority element, Mg, as well as with several other alloying elements present in the Mg-based alloys. Consequently, the Fe reinforcement can be dissolved in the high-temperature liquid, it would segregate together upon cooling, and subsequently solidify in the form of dendrites or particles, in a uniform fashion. This leaves behind a melt with a composition essentially identical to the original Mg-based BMG former. As such, Fe has little chance of reacting with the other elements to form brittle intermetallics, or of changing the composition of the base Mg alloy to degrade

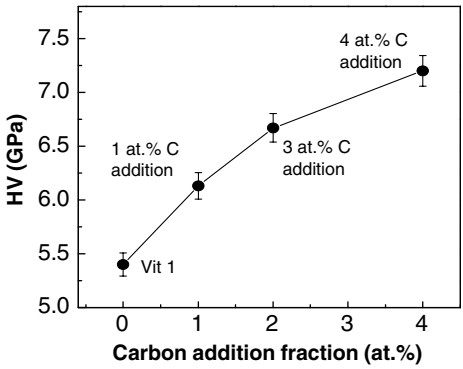

Fig. 8. A comparison of the Vickers hardness (H_v) changes with the increase of carbon content in the $Zr_{41}Ti_{14}Cu_{12.5}Ni_{10}Be_{22.5}$ BMG.

its good GFA. The uniform distribution of ductile Fe improves the plasticity and toughness of the alloy [145].

The BMGs have also been used as glassy matrix for particulate diamonds, filamentary SiC, TiC, WC, tungsten metal particles, and so on [1–4]. It is found that the mechanical strengthening in the composites obeys approximately the simple mixture rule that was commonly used to predict the properties of the metal–matrix composites [146]. The results indicate that the strengthening mechanism of the dispersed the second phase in BMGs may be similar to that of crystalline metal–matrix composites, which has been related to a high dislocation density in the matrix originating from differential thermal contraction, geometrical constraints during the processing. The strengthening could be obtained by hindering propagation of the cracks and shear bands in the glassy composites due to the existence of the crystalline reinforcement particles.

4.2. BMG–matrix composites with improved plasticity

One of the dreadful problems for the applications of BMG materials is the limited plasticity. In contrast to metallic glasses, useful crystalline metals exhibit substantial plastic strains following yielding under tension, and this results in high fracture toughness and impact resistance. One way to provide a global ductility to BMG is to produce a composite microstructure, consisting of crystalline and amorphous phase. The second crystalline phase distributed in the amorphous matrix may act as an initiation site of shear band resulting in multiple shear band formation throughout the specimen and confine the propagation of the shear band [57–59,139–141]. The effective way to obtain the composite microstructure is to *in situ* precipitate the ductile crystalline phase in the BMGs or to directly add the second ductile phase in the glassy matrix. Conner et al. [57] have prepared $Zr_{57}Nb_5Al_{10}Cu_{15.4}Ni_{12.6}$ BMG composites reinforced by metals or metal fibers or ceramic particles, such as W, WC, Ta and SiC. Their results show that the compressive strain to failure increases by more than 300% compared with the unreinforced BMG, and the fracture energy of the tensile samples increases by more than 50%. The increase in toughness comes from the particles restricting shear band propagation, promoting the generation of multiple shear bands and additional fracture surface area. Hays et al. [58] investigated the effect of *in situ* formed ductile dendritic precipitates dispersed homogeneously in the BMG matrix on the mechanical properties, the plasticity and the shear flow deformation of BMGs. Primary dendrite growth and solute partitioning in the molten state yields a microstructure consisting of a ductile crystalline Ti–Zr–Nb phase, with *bcc* structure, in a vit1 matrix. The dendritic microstructure of the Ti–Zr–Nb phase confines the propagation of individual shear bands, and play a key role in initiating the formation of multiple shear bands, and leads to over 8% of total strain (elastic and plastic) of the composites. The plastic strain to failure, impact resistance, and toughness of the metallic glass is dramatically increased [58]. The method is even extended to nanocrystalline metallic materials. An *in situ*-formed nanostructured matrix/ductile dendritic phase composite microstructure for Ti-base alloys, which exhibits up to 14.5% compressive plastic strain at room temperature [53]. The macroscopic plasticity of the centimeter-scale Ni-based metallic glass matrix composites is reinforced by 40% in volume fraction of brass fibers due to the formation of multiple shear bands, initiated from the interface between brass fiber and metallic glass matrix, as well as their confinement between the brass fibers [147].

The strength and ductility of the BMG can be enhanced by the *in situ* formation of nanoscale quasicrystalline phase in the glassy matrix. So far, the improvement of the mechanical properties by precipitation of the quasicrystalline phase has been reported in Zr-, Cu- and Ti-based BMG-forming alloys [148–150]. By controlling the preparation condition and composition modification, it has been found that the as-cast $Cu_{50}Zr_{50}$ alloy rod has a nanostructure consisting of a glassy phase containing fine crystalline particles with a size of about 5 nm. Because they contain a dispersion of embedded nanocrystals, the as-cast metallic glass rods has a high yield strength of 1860 MPa, a high Young's modulus of 104 GPa, and can sustain a compressive plastic strain at room temperature of more than 50%. The unusual compressive plastic strain is ascribed to the suppression of shear softening through nanocrystal coalescence [151].

4.3. BMG–matrix composites with unique physical properties

Since the low melting temperature and the high resistance against heterogeneous nucleation of crystals, the BMGs materials are good matrix materials for composites. This makes that the composite materials with unique properties could be obtained by mixing BMG matrix and novel materials with unique physical and chemical properties.

Carbon nanotubes (CNT), which is being called the ultimate fibers, possess not only extremely high elastic modulus and plasticity but also other unique physical properties [152]. The excellent mechanical properties and the predicted chemical stability that originates from their seamless cylindrical graphitic structure suggest that CNT might act as a novel material for preparing metallic glassy matrix composites, which might possess unique properties such as high strength, lightweight and stiff. Because the addition of CNT can act as the heterogeneous nucleation for degrading the GFA, the BMG matrix material must have the excellent GFA such as $Zr_{52.5}Cu_{17.9}Ni_{14.6}Al_{10}Ti_5$ BMG which has a critical cooling rate about 100 K. Another challenge is how to normally distribute the CNT in the glassy matrix without destroying the tube structure of the CNT.

Fig. 9 shows XRD patterns of the reinforced $Zr_{52.5}Cu_{17.9}Ni_{14.6}Al_{10}Ti_5$ BMG with 3 vol.% CNT addition, the $Zr_{52.5}Cu_{17.9}Ni_{14.6}Al_{10}Ti_5$ BMG and pure CNT powders. The curve of the composite shows a superimposition of broad maximum from the amorphous

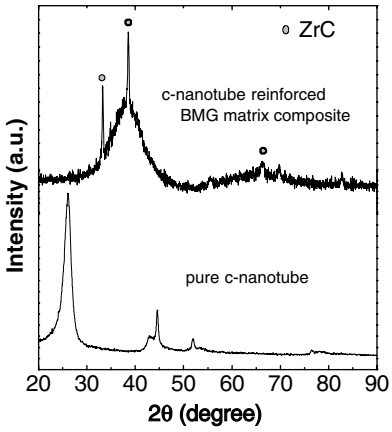

Fig. 9. XRD patterns of the pure CNTs and CNT reinforced BMG composites.

phase and several sharp peaks characteristic for a crystalline phase, suggesting that the presence of a mixture of the amorphous and a little crystalline phases. The position and the intensity of the crystalline peaks match exactly with that of ZrC carbide indicating that the part of carbon nanotubes have reacted with Zr and formed crystalline ZrC. The similar results by introducing carbon fibers or carbon element into BMG matrix have also been reported [54]. Some CNTs with obviously tubular structure can be observed in Fig. 10, which suggests that the CNTs have been distributed into the BMG matrix. HRTEM observation further confirms the mixture of CNTs with the BMG matrix. It is clearly seen that CNTs still keep good seamless cylindrical graphitic structure, implying that some CNTs in the BMG matrix still have original microstructure. The important reason for the distribution of CNTs into the glassy matrix is due to high thermal stability and the chemical stability of the CNT, and the low melting point (about 1100 K) and the strong GFA of the $Zr_{52.5}Cu_{17.9}Ni_{14.6}Al_{10}Ti_5$ alloy.

After the addition of CNT, the elastic moduli determined from acoustic measurements increase. The relative changes in E, bulk modulus K, shear modulus G and Debye temperature θ_D are 6.88%, 12.2%, 6.4%, 3.56%, respectively. The density decreased about 1.83%. This is due to the values of E of ZrC phase ($E = 390$ GPa) and CNTs (1.8 TPa) are much larger than that of the $Zr_{52.5}Cu_{17.9}Ni_{14.6}Al_{10}Ti_5$ BMG [152]. Even if 1 vol.% CNTs were kept in the BMG matrix after the interfacial reaction between carbon tubes and Zr, the theoretical value of E of the present composite is estimated to be 110 GPa according to the simple mixture rule. This value is very close to the experimental value (about 94.6 GPa) [56]. More carbon tube addition could greatly improve the mechanical properties of the Zr-based BMG.

The formation of the mixed structure of the residual CNTs and ZrC phase dispersing randomly in the BMG matrix indicates there are large amounts of new interfaces originating from the interfacial reaction between the added CNTs and the glass phase. This special structure causes a strong acoustic wave attenuation and absorption as shown in Fig. 11. Fig. 12 shows that the ultrasonic attenuation coefficients are very sensitive to the addition of CNTs, and the values of longitudinal and transverse ultrasonic attenuation (α_l and α_t) increase significantly with the increase of CNT addition. For 4 vol.% CNT addition, α_l is about 10 times and α_t is nearly 7 times larger than those of the undoped BMG, respectively. Even 1 vol.% CNT addition causes very large relative changes in α_l and α_t (440% and 255%, respectively). For more than 5 vol.% additions, the values of acoustic velocities could not be detected because ultrasonic attenuation is too strong so that no pulse echo is observed on the screen under applying experiment frequency. The above results imply that the addition of CNTs into the Zr-based BMG matrix causes strong ultrasonic attenuation and wave absorption. The strong absorption originates from the structural variation induced by adding CNTs into the BMG matrix [56]. The results show that the composites might have potential of application in the field of shielding acoustic sound or environmental noise.

Glassy metallic foam can be classified as the composites with BMG matrix formed by "adding" either open or closed porous into the BMGs [60,153–155]. The bulk glassy foam densities as low as 1.43 g/cm^3 are obtained, corresponding to a bubble volume fraction of 84%. The bubble diameter ranges from 25×10^{24} to 10×10^{23} m. The glassy foam's thermal stability is comparable to the bulk material [153]. Porous BMG were produced by water quenching a mixture of the Pd–Cu–Ni–P alloy liquid and solid salt (NaCl) in a silica tube, followed by leaching into water warmed at 353 K to eliminate the salt. To avoid

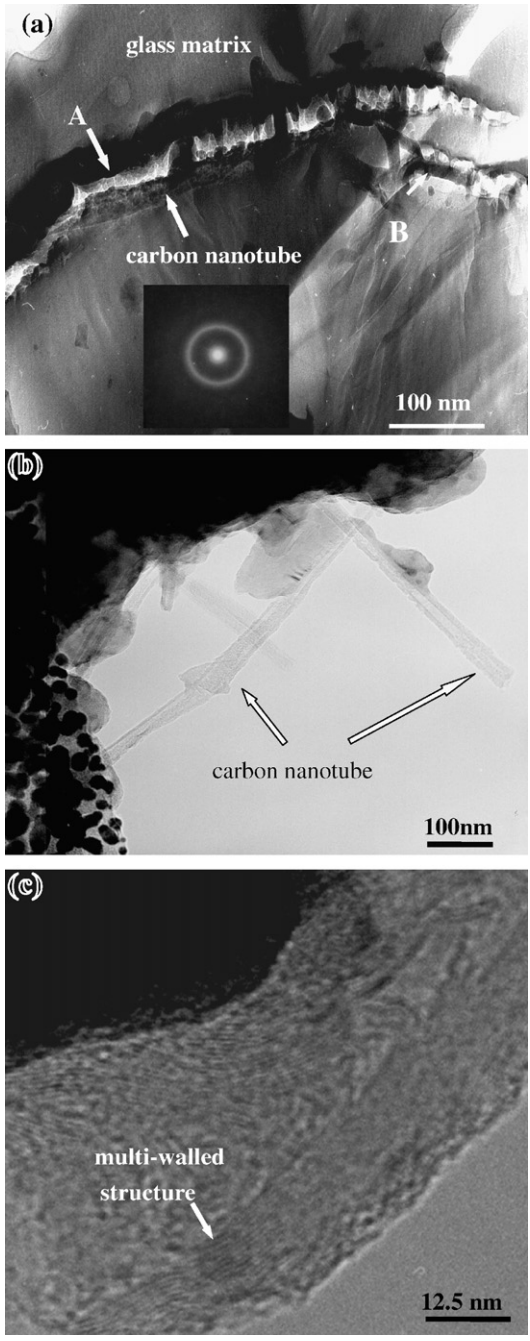

Fig. 10. Image (a) shows the typical TEM morphology of the microstructure of BMG composites containing CNT additions. Image (b) shows that the tubular shape of the added CNTs is BMG matrix, and the inset is the selected area diffraction pattern (SADP) of the matrix in the composite; and image (c) is the typical HRTEM morphology of the tubular shape of the added CNTs showing that the CNTs still keep their multiwalled structure after distributed into BMG matrix [56].

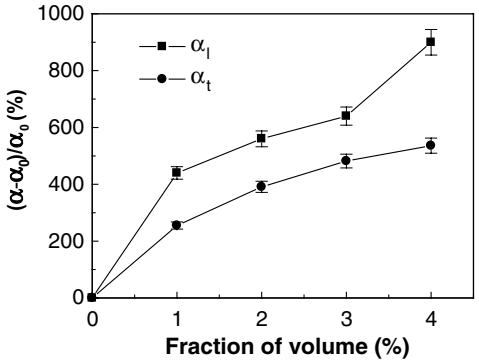

Fig. 11. Relative changes $[\Delta\alpha/\alpha_0 = (\alpha - \alpha_0)/\alpha_0]$ of the longitudinal and transverse ultrasonic attenuation (α_l and α_t) of Zr-based BMG composites with increasing volume fractions of CNT addition. (α_0 is attenuation coefficient of the undoped BMG; α is attenuation coefficient of composites) [56].

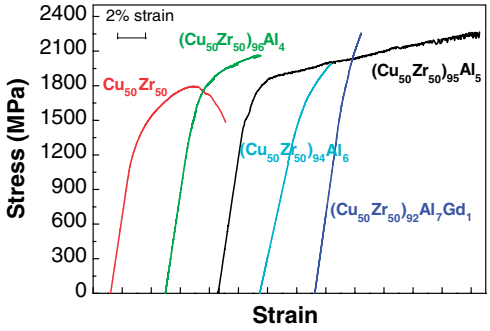

Fig. 12. Stress–strain curves of (a) $Zr_{50}Cu_{50}$, (b) $(Cu_{50}Zr_{50})_{96}Al_4$, (c) $(Cu_{50}Zr_{50})_{95}Al_5$, (d) $(Cu_{50}Zr_{50})_{94}Al_6$ and (e) $(Cu_{50}Zr_{50})_{92}Al_7Gd_1$ under compression at a strain rate of 8×10^{-4} s^{-1}. The $(Cu_{50}Zr_{50})_{95}Al_5$ BMG shows a highly "work hardenable" metallic glass up to 18% strain.

crystallization, the excellent glass former alloy such as PdNiCuP is usually chosen as a foaming material. Glassy foams have many interesting combinations of physical properties. They exhibit lower Young's modulus, lower yield strength, much higher absorption energy, being significantly different from those for the pore-free BMGs. Especially, the BMG foams can achieve very high compressive and bending ductility (comparable to ductile crystalline metallic foams), in sharp contrast to the brittle behaviors of BMGs. The unique mechanical characteristics combined with high absorption energy ability indicate the possibility of future uses as a new type of structural and functional materials.

Many reports, for example see Refs. [156–159], indicate that adding small amounts of Ag, Pd, Ti, or Nb to ZrNiCuAl glass-forming alloys promotes formation of icosahedral phases in the glassy alloys due to a nearly zero or positive heat of mixing with at least one of the major alloying elements, such as Ni. The precipitation of an icosahedral quasicrystal can significantly improve the ductility of the BMGs [156–159].

Soft magnetic glassy Fe-based alloys have attracted great interest recent years because they exhibit extremely low values of coercive field (~1 A/m) in the optimum

nanocrystalline state [160]. These materials are characterized by a microstructure consisting of two phases: nanocrystalline grains embedded in a residual glassy matrix. The typical size of the nanocrystals is around 10–15 nm, showing a random orientation of their easy axis. The soft magnetic behavior in these alloys arises from the average of the magnetocrystalline anisotropy of the randomly oriented nanocrystalline grains by the exchange interactions [161]. The excellent soft magnetic properties of these biphase materials are related to the strong coupling between the crystalline grains, which suggest a relevant role of both, the magnetostatic interactions and the formation of these coupled nanocrystals.

The effects of the substitution of Fe atoms by additional alloying elements on its magnetic properties have been investigated. The minor alloying Co and Al as substituting elements led to a significant decrease in the minimum of coercivity as well as in the magnetostriction values achieved after partial devitrification [162,163]. The substitution of Fe atoms by Ni ($Ni_xFe_{73.5-x}Si_{13.5}B_9Nb_3Cu_1$) reveals an enhancement of the nanocrystallization of the material, favored by the presence of a third magnetic element. Therefore, the proper addition opens a field in the optimization of the soft magnetic characteristics of metallic glassy alloys [164]. The addition of 2.5 at.% Si is found to be effective for the increase of the saturation magnetization and decrease of the coercive force for the $Fe_{77}Ga_3P_{12-x}C_4B_4Si_x$ and $Fe_{78}Ga_2P_{12-x}C_4B_4Si_x$ bulk glassy alloys [165].

5. Enhance and tune properties by minor additions

Previous studies show that the elastic constants (M) of most BMGs can be calculated in the form [112,166,167]:

$$M^{-1} = \Sigma f_i \cdot M_i^{-1}, \tag{1}$$

where M_i and f_i denote any elastic constant and the atomic percentage of the constituent element, respectively. The calculated elastic constants of the BMG in terms of the empirical equation (1) are roughly in agreement with the values obtained by using ultrasonic mouthed or other methods [112,166,167]. On the other hand, the experimental data reveal striking systematic correlations between linear elastic constants, mechanical properties, plastic yielding of the glass, crystallization temperature, the glass transition temperature, and rheological properties of the glass-forming liquid [8,91,166–171]. These correlations indicate the technological and scientific importance of the elastic properties of a glass, and mean that controlled elastic moduli of the alloy can be used to control the properties of the BMGs. Therefore, the established correlations, associated with elastic moduli, and since the moduli of glasses scale with those of their elemental components, provide useful guidelines for minor addition by selection of proper minor alloying material with suitable elastic moduli [8,91,166–170]. In fact, based on the correlations, minor addition is used to control the structure and properties of BMGs.

5.1. Enhance the properties

5.1.1. Enhance the plasticity and strength of BMGs

Based on the binary $Zr_{50}Cu_{50}$ alloys, a new class of inherently ductile metallic glasses in a simple ternary Zr–Cu–Al alloy with relatively high glass transition temperature has been discovered [66,172,173]. Fig. 12 shows the stress–strain curves of $Zr_{50}Cu_{50}$ and $(Cu_{50}Zr_{50})_{100-x}Al_x$ ($x = 4$, 5, 6) $(Cu_{50}Zr_{50})_{92}Al_7Gd_1$ BMGs. The room temperature

compression test results for $Cu_{50}Zr_{50}$-based alloys are also listed in Table 5. The ultimate compression stress σ_{max} of the $Zr_{50}Cu_{50}$ is 1794 MPa with strain of 5.7%, then the stress decreases with further increasing strain and final failure occurs at fracture strain $\varepsilon_f = 7.9\%$. The yield strength, yield strain ε_y, σ_{max}, and ε_f and of $(Cu_{50}Zr_{50})_{100-x}Al_x$ BMGs are markedly changed by Al addition as shown in Fig. 13 and Table 5, and a suitable Al addition (Al = 5 at.%) σ_y increases to 1573 MPa and is considerably higher than the value of $Zr_{50}Cu_{50}$. More importantly, after yielding, $Zr_{47.5}Cu_{47.5}Al_5$ exhibits a strong increase of the stress with further increase in strain representing a "work hardening" behavior up to 18% strain. The maximum compressive stress of $Zr_{47.5}Cu_{47.5}Al_5$ was measured to be 2265 MPa. It is very clear that there is an increase of the flow stress after yielding after suitable Al addition [66]. The "work-hardening" capability and plasticity of this class of metallic glass is attributed to the minor addition induced unique structure correlated with atomic-scale inhomogenieties leading to an inherent capability of extensive shear band formation, interactions and multiplication of shear bands [66]. Similar effect of plasticity enhancement has also been obtained by addition of Ti in CuZr metallic glasses [67], addition of Ta in ZrCuNiAl alloy [68], and additions of Hf, Zr, Si in $Ti_{50}Cu_{50}$-based metallic glasses [69].

Woehler curves of $Zr_{50}Cu_{40}Al_{10}$ and $Zr_{50}Cu_{30}Ni_{10}Al_{10}$ BMGs using a rotating-beam fatigue test have been measured to evaluate the effect of addition Ni on fatigue strength [174]. The fatigue limit was increased from 250 MPa to 500 MPa by adding Ni instead of Cu to the $Zr_{50}Cu_{40}Al_{10}$ BMG. The $Zr_{50}Cu_{40}Al_{10}$ BMG exhibits wider fatigue-fractured

Table 5
Room temperature compression test results for $Cu_{50}Zr_{50}$-based alloys with different additions

Alloy	E (GPa)	σ_y (MPa)	ε_y (%)	σ_{max} (MPa)	ε_f (%)
$Cu_{50}Zr_{50}$	84	1272	1.7	1794	7.9
$(Cu_{50}Zr_{50})_{94}Al_4$	88.7	1611	2.1	2068	5.4
$(Cu_{50}Zr_{50})_{95}Al_5$	87	1537	2.0	2265	18.0
$(Cu_{50}Zr_{50})_{94}Al_6$	92.4	1636	2.1	1999	2.8
$(Cu_{50}Zr_{50})_{93}Al_7Gd_1$	90.6	1774	2.0	2249	1.1

The minor addition has significant effects on the mechanical properties: Young's modulus E, yield stress σ_y, yield strain ε_y, ultimate compression stress σ_{max}, and fracture strain ε_f.

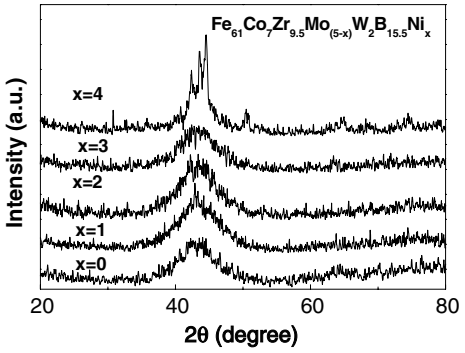

Fig. 13. XRD patterns of the as-cast $Fe_{61}Co_7Zr_{9.5}Mo_{5-x}Ni_xW_2B_{15.5}$ ($x = 0$, 1, 2, 3, and 4) alloys.

region with striation-like marks than that of the $Zr_{50}Cu_{30}Ni_{10}Al_{10}$ BMG. Additive Ni element limits the fatigue-fractured region to half of the whole fractured surface. Especially, the fatigue fracture toughness decreases suddenly around 103–104 cycles, similar to the Woehler curves. The significant decrease of fatigue–fracture toughness originates from embrittlement/hardening in front of the fatigue crack tip during fatigue test induced by addition [174].

How the plasticity of amorphous steel FeMoCB change by tuning the elastic properties (Poisson's ratio or G/K) of the alloy via changes of the additional rare earth elements has been recently studied [175]. The sensitivity of elastic properties to small compositional variation has enabled the accurate determination of the transition from plasticity to brittleness in the amorphous steel.

5.1.2. Stabilize the BMGs

The addition of Nb and Ta elements can stabilize the Zr-based BMGs. The Nb and Ta have similar structural properties to those of Ti and Ni, but Nb and Ta have much higher melting temperatures. Therefore the substitution of Ti and Ni with Nb and Ta can improve the thermal stability of the BMG without impairing the GFA of the alloy [33]. Both T_g and T_x of the $Zr_{48}Nb_8Cu_{14}Ni_{12}Be_{18}$ BMG have higher values than that of the $Zr_{41}Ti_{14}Cu_{12.5}Ni_{10}Be_{22.5}$ BMG, meaning the higher thermal stability. Nb addition can also improve the thermal stability of Zr-based BMGs. Ta can substitute of Ti in the Zr/Be-based BMGs of the alloys. Furthermore, Ta is more effective to increases the thermal stability without significantly change the GFA comparing with Nb [33]. Additional metals with higher melting temperature are feasible way to improve the thermal stability of BMGs [24,25,43].

5.1.3. Improve the magnetic properties of BMGs

The development of soft magnetic metallic glasses with large GFA has become an important research topic in recent years because the soft magnetic properties are promising for many applications such as magnetic conductor and magnetic elements [1–3]. Recently, Fe-based BMGs were obtained by a copper mold casting technique at cooling rate as low as 10^2 K/s [23,72,73,86,87]. These Fe-based BMGs exhibit the highest thermal stability ($T_g = 898$ K, and $T_x = 950$ K), the high corrosion resistance and the highest strength (the compressive strength $\sigma = 3800$ MPa, and Vickers hardness $H_v = 13.6$ GPa) among known Fe-based alloys [23]. Unfortunately, the soft magnetic properties of the BMG are not as good as that of other Fe-based BMGs. Hence, it is vital to further improve its magnetic properties so that it is more viable for commercialization and future applications.

The minor addition can be used for improving the magnetic properties of the Fe-based BMG [62]. A small amount of Ni addition can spectacularly improve the soft magnetic property as well as the electrical behavior of the $Fe_{61}Co_7Zr_{9.5}Mo_5W_2B_{15.5}$ BMG without markedly deteriorating its high GFA. The XRD, DTA and TEM results of the as-cast $Fe_{61}Co_7Zr_{9.5}Mo_{5-x}Ni_xW_2B_{15.5}$ ($x = 0$–4 at.%) alloys, as shown in Fig. 14, indicate that Ni addition up to 3 at.% does not deteriorate the GFA of the alloy. The hysteresis loops of the $Fe_{61}Co_7Zr_{9.5}Mo_{5-x}Ni_xW_2B_{15.5}$ alloys with different Ni contents are displayed in Fig. 14. The BMG without Ni addition does not show soft magnetic behavior. The shape of the hysteresis loops (Inset (a) shows the enlarged hysteresis loop) for the BMG indicates that it is typical of magnetic material with large anisotropy field. However, with only

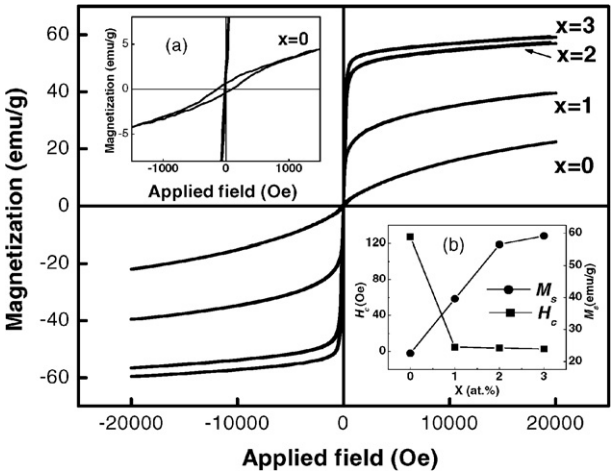

Fig. 14. Hysteresis loops measured for the $Fe_{61}Co_7Zr_{9.5}Mo_{5-x}Ni_xW_2B_{15.5}$ ($x = 0$, 1, 2, and 3) alloys. The inset (a) shows the enlarged hysteresis loops. The inset (b) shows the variation of M_s and H_c of the as-cast alloys as a function of Ni addition [62].

1 at.% Ni addition, the alloy exhibits soft magnetic behavior. For $x = 2$, and 3, the soft magnetic property of the alloy is much improved. The changes of coercivity, H_c and saturation magnetization, M_s as a function of Ni content are shown in the inset (b) of Fig. 14. The H_c decreases rapidly from 127.0 to 4.8 Oe with 1% Ni addition, and then further decreases to 3.0 Oe for 3% Ni addition. The M_s increases from 22.5 to 59.1 emu/g when Ni content reaches 3%. The Ni addition decreases the antiferromagnetic interaction and increases the exchange length, and then leads to the increases of M_s and the decrease of H_c [62].

The rare earth elements are magnetic due to their incompletely filled inner f electron shells. Hence, minor additions of magnetic rare earth elements may affect not only the GFA of bulk glass-forming alloys but also their magnetic properties. Minor addition of Dy in $Fe_{70-x}Dy_xZr_8Mo_5W_2B_{15}$ ($0 < x < 5$ at.%) alloys has been studied using *dc* and *ac* susceptibility measurements. A re-entrant spin glass behavior is observed in the BMGs and the phenomenon is ascribed to Dy minor addition induced site frustration. The magnetic properties of the BMGs are found to be tunable by appropriate selection of the Dy content, and the schematic magnetic phase diagram as a function of Dy content is derived and shown in Fig. 15 [123].

The influence of Co addition on the magnetic entropy change of the FeCoSiAlGaPCB alloys has been studied. This compositional modification can displace the temperature of the peak entropy change closer to room temperature [176].

5.1.4. Enhance the corrosion resistance of BMGs

The effects of the addition of a small amount of elements such as Cr, Mo, Nb, Hf or W on corrosion resistance of the BMGs were investigated by means of electrochemical polarization and weight loss measurements [177,178]. Electrochemical measurements on BMGs were conducted in 1 N H_2SO_4 and 1 N NaOH aqueous solutions, respectively, at room temperature. It is showed that the $Cu_{47}Zr_{11}Ti_{34}Ni_8$ BMG with a small amount of Cr,

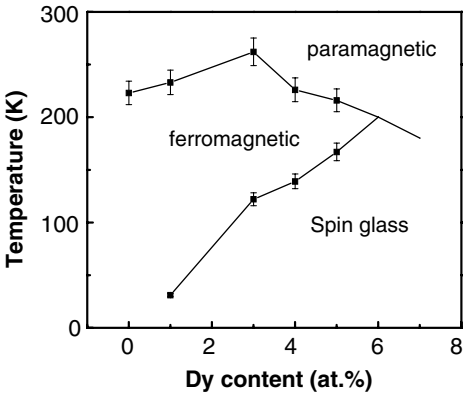

Fig. 15. Magnetic phase diagram for the $Fe_{70-x}Dy_xZr_8Mo_5W_2B_{15}$ ($0 \leqslant x \leqslant 5$) BMGs derived from the temperature-dependent AC susceptibility at 10 Oe and 1000 Hz.

Mo or W exhibits a superior corrosion resistance in the two electrolytes as compared with the base alloy. The $(Cu_{47}Zr_{11}Ti_{34}Ni_8)_{99.5}Mo_{0.5}$ BMG exhibits the greatest corrosion resistance, as indicated by the lowest passive current density and the lowest corrosion rate. The results demonstrate that the corrosion resistance of Cu-based BMGs with Cr minor addition is much better than that of the stainless steel. The additions of Nb and Hf (1–5 at.%) can significantly enhance the corrosion resistance of the $Zr_{65}Cu_{17.5}Ni_{10}Al_{7.5}$ BMG indicated by a remarkable increase in corrosion potential and pitting potential [177,178]. XPS analysis revealed that the passive film formed after anodic polarization was enriched in aluminum oxide and depleted in phosphate ions for the BMGs containing Nb, which accounted for the improvement of corrosion resistance. On the other hand, metal–ion release of different BMGs were determined in PPb (ng/mL) level with inductively coupled plasma mass spectrometry (ICP-MS) after being immersed in artificial body fluid at 37 °C for 20 days. It is found that the addition considerably reduces the ion release of all kinds of metals of the base system. This is attributed to the promoting effect of minor addition on a rapid formation of highly protective film [177,178].

5.2. Tune the properties

Microstructure and properties controlled bulk glassy materials are expected to have application potentials. However, the microstructural control in the metallic alloys is a longstanding problem due to the high nucleation and growth rates and instability of their supercooled liquid state. The BMG-forming alloys with a very stable supercooled liquid state and high thermal stability against crystallization offer a large experimentally accessible time and temperature window for developing some methods (such as controlled solidification, high annealing, pressure [1–3]) to tailor their properties through controlling of the microstructure or the nucleation and growth in supercooled liquid state.

The element addition could provide a way to this open issue. It is found that the microstructure and property can be manipulated in the rare-earth-based BMGs-forming alloys (e.g. Pr- and Nd-based alloys) by varying Fe addition. By varying Fe content, the microstructure of the Nd- and Pr-based alloys change progressively from full glassy state to

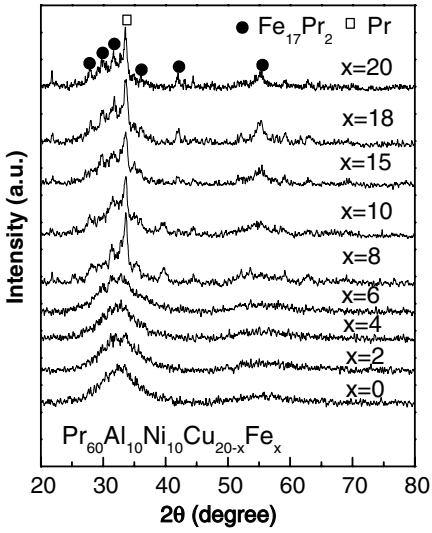

Fig. 16. XRD patterns for the as-cast $Pr_{60}Al_{10}Ni_{10}Cu_{20-x}Fe_x$ alloys with different Fe additions.

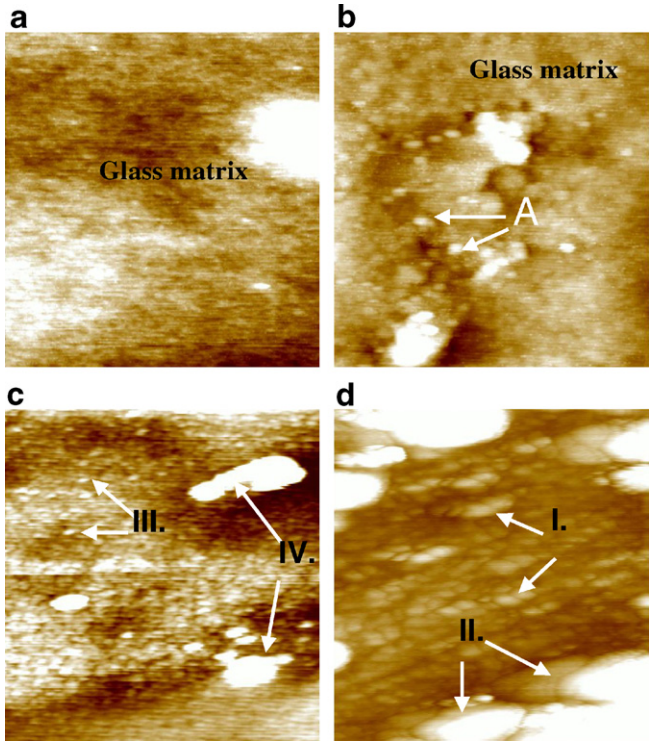

Fig. 17. AFM images (1 μm × 1 μm) of the as-cast $Pr_{60}Al_{10}Ni_{10}Cu_{20-x}Fe_x$ ($x = 4$, 10, 15 and 18) alloys. (a) $x = 4$; (b) $x = 10$; (c) $x = 15$; (d) $x = 18$. The ultrafine nanocrystalline grains are indicated by marker *A*, the regions marked by *B* originate from the overlapping nanocrystalline grains with different random orientations [65].

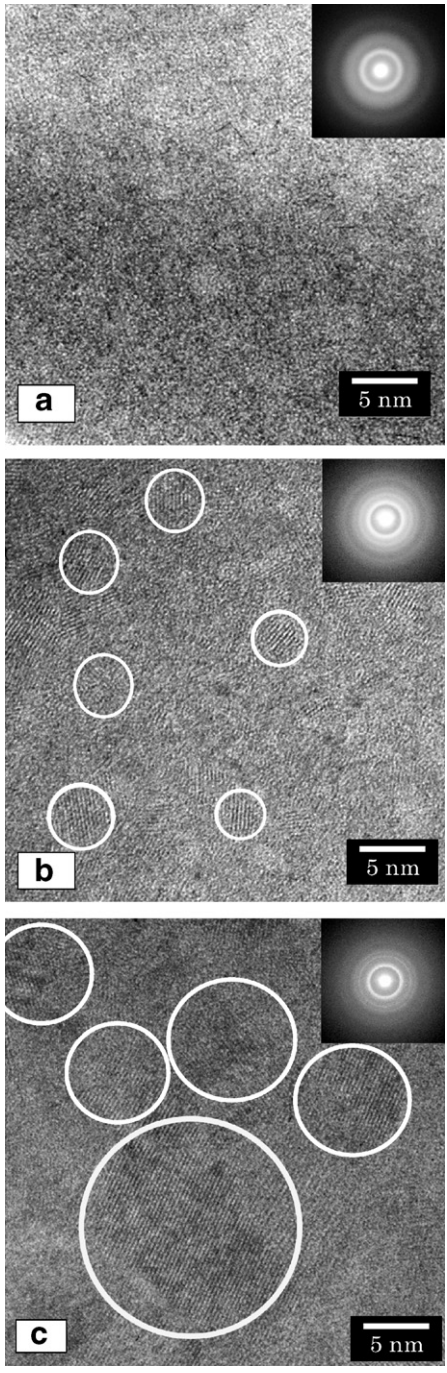

Fig. 18. High-resolution TEM image of the as-cast $Nd_{60}Al_{10}Ni_{10}Cu_{20-x}Fe_x$ ($x = 0$, 4, 20) alloys. (a) for the alloy with $x = 0$; (b) for the alloy with $x = 4$; and (c) for the alloy with $x = 20$. It can be clearly seen that Fe additions result in the precipitation of nanocrystalline phases with increasing average size and volume fraction upon Fe content [63].

composite with nanocrystalline particles in the glassy matrix, and finally change into a full nanostructure. The structural change is accompanied with the magnetic property changes gradually from paramagnetic to hard magnetic [63,65].

Fig. 16 shows the structural change with increasing Fe content in the $Pr_{60}Al_{10}Ni_{10}Cu_{20-x}Fe_x$ alloys. It can be seen that with increasing Fe content the intensity of the crystalline peaks increases meanwhile the intensity of the diffused amorphous peak decreases. The XRD result demonstrates that the Pr-based alloys show a pronounced and progressive microstructure changes from full glassy state to nanostructure upon Fe addition. The atomic force microscopy (AFM) (see Fig. 17) (1 μm × 1 μm) of the as-cast $Pr_{60}Al_{10}Ni_{10}Cu_{20-x}Fe_x$ ($x = 4$, 10, 15, 18) alloys both on the surface and in cross-section, and the HRTEM images shown in Fig. 18 confirm that the precipitation of nanocrystalline phases with increasing average size and volume fraction upon Fe content.

The DSC traces (Fig. 19) also exhibit the microstructural evolution of the $Pr_{60}Al_{10}Ni_{10}Cu_{20-x}Fe_x$ alloys. The result is in good agreement with that of XRD and AFM analysis. The melting process of these alloys is also sensitive to Fe content. For the alloys without Fe addition, the melting is eutectic. With increasing Fe content, the composition of the alloy gradually deviates from the eutectic composition that is normally the best glass-forming composition for an alloy, resulting in the deterioration of the GFA. The mutually repulsive interaction of Fe and Pr (or Nd) with positive heat of mixing leads to clustering in the alloys [75], the clustering or phase separation already present in the liquid state is frozen and retained in alloys. In addition, Fe element is expected to cause further increase of melt viscosity in the supercooled liquid according to "confusion principle" [1], and the inhibition to the growth of the kinetically favored phases becomes stronger in the viscous melt. These facilitate the microstructure of the alloys changes gradually from amorphous to nanocrystalline state with Fe doping.

The additions change the magnetic properties. The room temperature M–H hysteresis loops measured at an applied field of 800 kA m^{-1} for the $Pr_{60}Al_{10}Ni_{10}Cu_{20-x}Fe_x$ alloys are

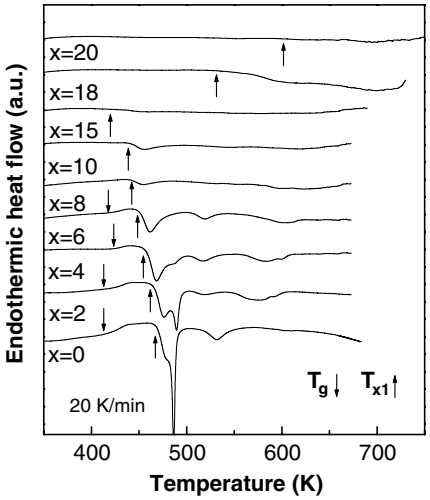

Fig. 19. DSC curves show the crystallization process of $Pr_{60}Al_{10}Ni_{10}Cu_{20-x}Fe_x$ ($x = 0$, 2, 4, 6, 8, 10, 15, 18, and 20) alloys. The scanning rate is 20 K/min [65].

shown in Fig. 20(a). Fig. 20(b) gives the variation of coercivity, H_c, remanence, M_r and maximum energy product, $(BH)_{max}$ of the alloys upon Fe content. All the H_c, M_r, and $(BH)_{max}$ increase firstly with increasing Fe content, and reach maximum values simultaneously around $x = 10$, and then decrease with further increase of Fe content. The Pr-based alloys changes progressively from paramagnetic to hard magnetic with Fe doping, and the doping approach allows the magnetic properties of the alloys to be easily tuned according to the specific applications, such as patterned magnetic nanostructures, which are required in the field of ultrahigh density magnetic recordings and submicron magnetoelectronics devices [65].

Fig. 21(a) and (b) show the simultaneously obtained (10×10)-μm AFM (left) and MFM (right) images of the samples ($x = 4$, 18), the inset (1 μm × 1 μm) with high magnification provides more additional details. It can be seen that the MFM images are characterized by darker areas adjacent with bright areas in submicron scale and in random distribution. The obvious addition-induced magnetic domain structure was observed in the alloys, which shows the direct experimental evidence for the existence of exchange-coupling interaction in nanocrystalline phases [114]. For the Fe-poor alloy ($x = 4$), the

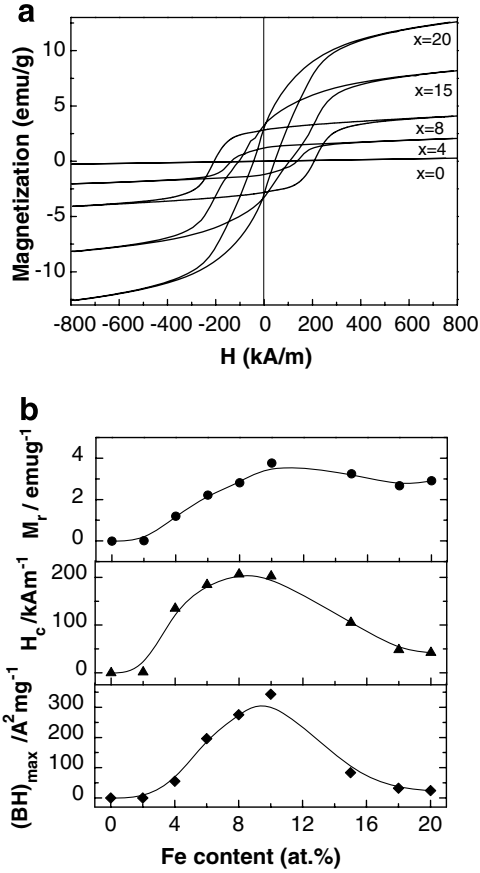

Fig. 20. (a) Hysteresis M–H loops of the as-cast $Pr_{60}Al_{10}Ni_{10}Cu_{20-x}Fe_x$ ($x = 0$, 4, 8, 15, 20) alloys. (b) The variation of H_c, M_r and $(BH)_{max}$ as a function of Fe content [65].

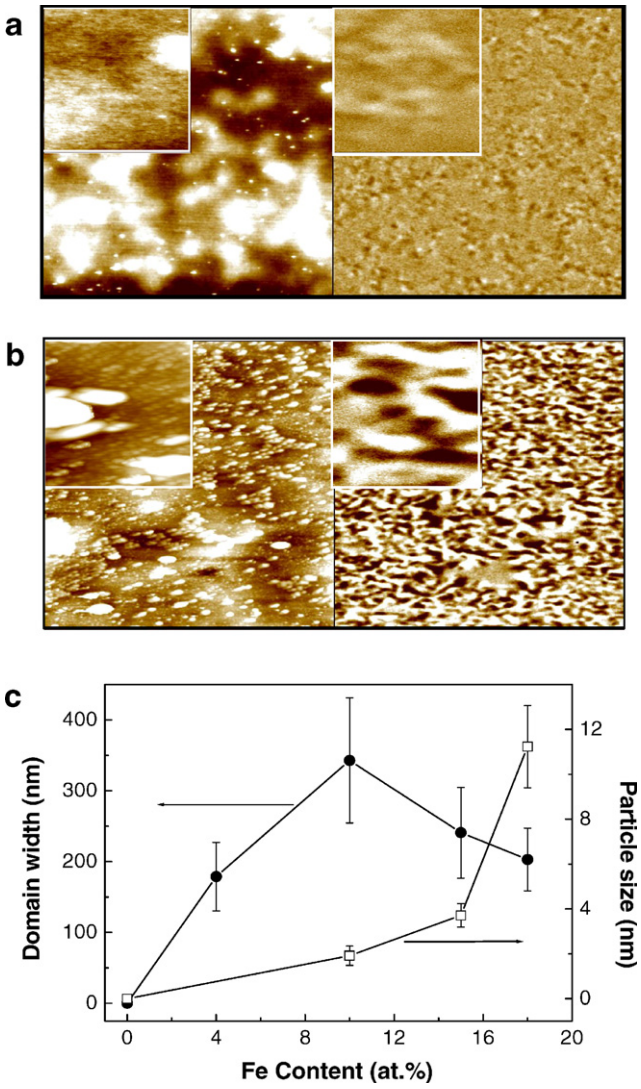

Fig. 21. Simultaneously obtained the typical (10 × 10)-μm AFM (left) and MFM (right) images of the as-cast (a) $x = 4$, and (b) $x = 18$ $Pr_{60}Al_{10}Ni_{10}Cu_{20-x}Fe_x$ alloys, the inset shows the images (1 μm × 1μm) with high magnification. (c) The variation of the domain width and grain size vs. Fe content [65].

magnetic nanoparticles is too small to be detected by XRD and AFM. Due to the interparticle exchange coupling, the nanoparticles with similar magnetic orientation are aligned to form the large-scale domains. The domain width and grain size versus Fe content are summarized in Fig. 21(c), and the variation in domain width as a function of Fe doping shows the similar trend to the coercivity.

In addition, the mechanical properties of the alloys can also be controlled with addition-induced structural evolution. The relative changes of the elastic moduli as a function of Fe content are presented in Fig. 22. All of the properties exhibit dramatic changes at 6%, and the E and G show a similar doping-dependence and almost the same relative

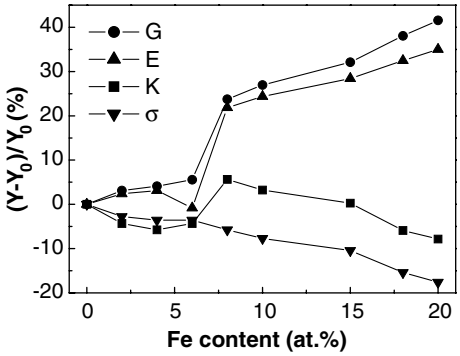

Fig. 22. The relative changes $\Delta Y/Y_0 = (Y - Y_0)/Y_0$ of variation of E, G, K and σ with the Fe content for the as-cast $Pr_{60}Al_{10}Ni_{10}Cu_{20-x}Fe_x$ ($x = 0$, 2, 4, 6, 8, 10, 15, 18, and 20) alloys. Y_0 and Y stand for the properties of glass state and various doping states of the alloys, respectively.

variation. The Fe addition can significantly increase the elastic moduli (more than 20% in increase for E and G with 8% Fe addition). The addition-dependent mechanical properties are ascribed to the progressive ordering as the BMG stepwise undergoes nanocrystalline formation [179,180]; and the dramatic changes at 6% roughly correspond to the onset of the precipitation of the nanocrystalline phases in the alloy; when the Fe content is larger than 8%, the E and G show a nearly linear increasing with Fe content, which is corresponding to the gradual growth of the nanocrystalline.

6. Some interesting phenomena induced by minor additions

6.1. Obtaining new BMGs systems based on binary BMGs by minor additions

Recently, some simple binary alloys such as NiNb [181,182], CaAl [183], PdSi [184], AlGe [185], CuZr [166,167,186–188] and CuHf [188] BMGs with the diameter up to 2 mm were produced. Based on these developments, minor addition was effectively performed on these binary BMGs to develop new BMGs with high GFA and unique properties. Fig. 23 shows an example for exploring new BMGs based on the $Cu_{50}Zr_{50}$

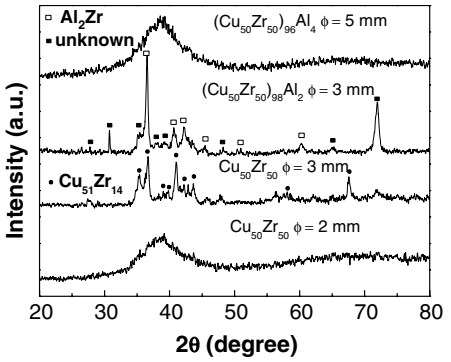

Fig. 23. XRD patterns of the as-cast rods of $Cu_{50}Zr_{50}$ and $(Cu_{50}Zr_{50})_{100-x}Al_x$ (at.%). The diameters of the rods are indicated and the phases giving rise to the Bragg peaks are identified as far as possible [173].

BMG. The critical diameter of the as-cast amorphous CuZr rod is 2 mm. When the diameter is larger than 3 mm, the alloy shows crystalline peaks, which are mainly corresponding to the crystalline $Cu_{51}Zr_{14}$ phase as marked in Fig. 23 (A small fraction of an unidentified phase is also found) [166,167]. This result indicates that the crystalline $Cu_{51}Zr_{14}$ phase is the main competing phase of the amorphous phase during solidification. With small (2 at.%) Al addition, the precipitation crystalline phases are obviously changed, and crystalline $ZrAl_2$ phase and other unknown phases form, which indicating the distinct role of Al in varying phase formation and evolution during solidification. When 4% Al is added, the full amorphous rod can be produced up to 5 mm at least. For the alloy with 4% Al addition, the critical cooling rate R_c drops from 250 K/s for the $Cu_{50}Zr_{50}$ BMG to about 40 K/s. With addition of aluminum to this alloy, the GFA is clearly increased. Fig. 24 presents XRD patterns of the as-cast $(Cu_{50}Zr_{50})_{100-x}Al_x$ ($x = 4$, 6, 8, and 10) alloys with different Al additions. The alloy containing 8% Al is of the best GFA in the alloy series. The critical diameter of the BMG decreases to 3 mm when Al further increases to 10%. The proper Al addition content range is $2 < x < 10$ at.%. DSC curves in Fig. 25 shows that

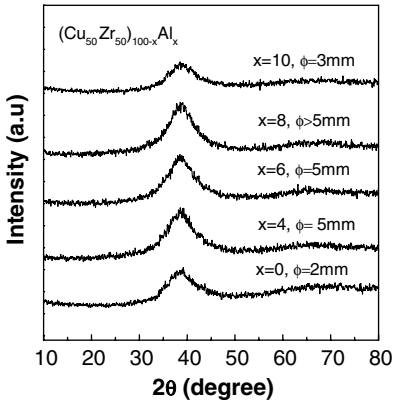

Fig. 24. XRD patterns of the $(Cu_{50}Zr_{50})_{100-x}Al_x$ ($x = 0$, 4, 6, 8, and 10) alloys.

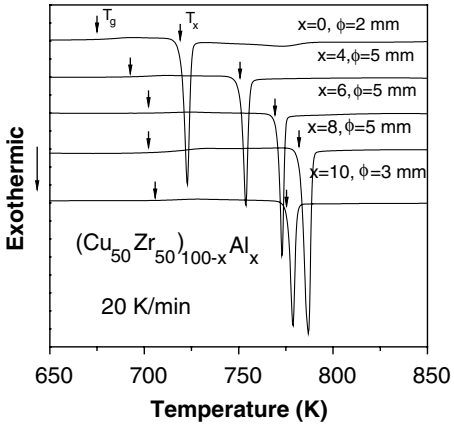

Fig. 25. DSC curves of the $(Cu_{50}Zr_{50})_{100-x}Al_x$ ($x = 0$, 4, 6, 8, and 10) alloys.

Al addition dramatically enhances the thermal stability of the $(Cu_{50}Zr_{50})_{100-x}Al_x$ ($x = 0$, 4, 6, 8, and 10) BMGs. With 4 and 8% Al addition, the T_x is increase about 34 and 66 K, respectively. Al addition makes both T_m and T_l of the $(Cu_{50}Zr_{50})_{100-x}Al_x$ ($x = 0$, 4, 6, 8, 10) alloys markedly decrease as shown in Fig. 26. But the melting behavior has not been changed for all of the alloys. The ΔT and T_{rg}, which are two critical parameters in evaluating the GFA of an alloy, both significantly increase from 47 K and 0.55 to 82 K and 0.61 when Al content x changes from 0 to 8, respectively, further confirming the critical role of Al addition in the improvement of the GFA.

Other elements can be added to the BMG-forming alloys to further increase the GFA. When 1% Gd is further added, the fully amorphous $(Cu_{50}Zr_{50})_{92}Al_7Gd_1$rod is obtained at least in 10 mm [37]. The sample is still composed of main glassy phase when the diameter increases to 12 mm. The R_c for the $(Cu_{50}Zr_{50})_{92}Al_7Gd_1$ is estimated to be 10 K s^{-1}. Fig. 27 shows the picture of the obtained $Cu_{50}Zr_{50}$ (2 mm), $(Cu_{50}Zr_{50})_{96}Al_4$ (5 mm) and $(Cu_{50}Zr_{50})_{92}Al_7Gd_1$ (8, 12 mm) BMGs. Their as-cast surfaces are all smooth and lustrous and no obvious volume shrinkage can be seen, implying these alloys have good castability and the disordered structure of their liquids can be readily arrested in solid state. Fig. 28 shows critical diameter, d of the $(Cu_{50}Zr_{50})_{100-x}Al_x$ and $(Cu_{50}Zr_{50})_{93-y}Al_7Gd_y$ BMGs as a function of the contents of Al and Gd. The $(Cu_{50}Zr_{50})_{100-x}Al_x$ alloys have the biggest critical dimension of 5 mm and do not show obvious change for 4–8 at.% Al addition; and that $(Cu_{50}Zr_{50})_{93-y}Al_7Gd_y$ is about 10 mm as Gd content in 1–3 at.%. More Al (>8%) and Gd (>3%) additions markedly decrease the GFA. The results indicate the GFA is quite sensitive to the quantity of the microalloying. More than 2% Gd addition does not further increase the GFA and even has negative effect.

Fig. 29(a) shows the DSC curves of the $Cu_{50}Zr_{50}$ and the samples microalloyed with Al and Gd. Fig. 29(b) presents the DTA curves exhibiting the melting process of these alloys. Especially, the melting of all of the alloys has a wide and complex process with several endothermic events, which imply the compositions are far from the eutectic point. The microalloying makes the liquid temperature T_l decrease from 1219 (for $Cu_{50}Zr_{50}$) to 1139 K (for $(Cu_{50}Zr_{50})_{92}Al_7Gd_1$) but the complex melting process has not been significantly changed. Good GFA normally associates with eutectics [1–3], but the additional alloys do not coincide with a deep eutectic in the equilibrium phase diagram. The obvious

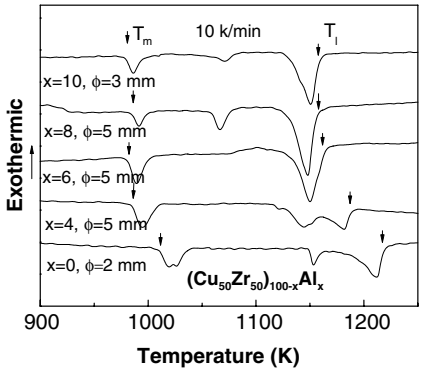

Fig. 26. DTA curves of the $(Cu_{50}Zr_{50})_{100-x}Al_x$ ($x = 0$, 4, 6, 8, and 10) alloys.

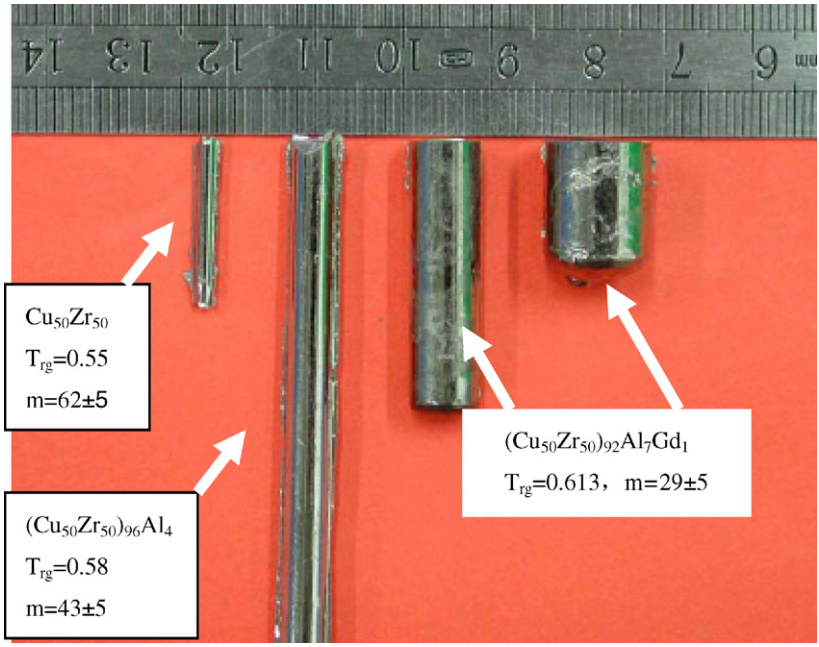

Fig. 27. The picture of the BMG samples: $Cu_{50}Zr_{50}$ (2 mm), $(Cu_{50}Zr_{50})_{96}Al_4$ (5 mm) and $(Cu_{50}Zr_{50})_{92}Al_7Gd_1$ (8 and 12 mm).

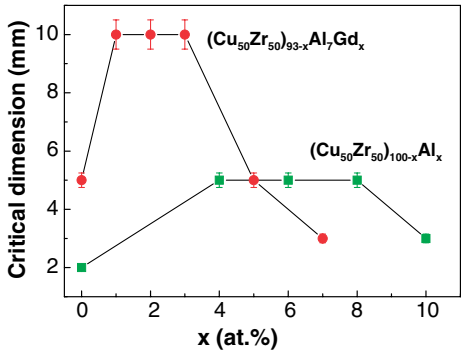

Fig. 28. The critical diameter of the $(Cu_{50}Zr_{50})_{100-x}Al_x$ and $(Cu_{50}Zr_{50})_{93-y}Al_7Gd_y$ BMGs as a function of Al and Gd microalloying contents. The figure illustrates the dramatically increase of the GFA of the alloy with minor addition.

increase of T_{rg} from 0.550 (CuZr alloy) to 0.613 (CuZrAlGd) confirms the great effect of the trace additions on the GFA.

Based on the binary NiNb, CuHf, PdSi, and CaAl BMGs, the NiNbSn [83], CuHfZr [3,4], PdSiCu [184], and CaAlCu(Ag, Mg, Zn) BMGs [183] with excellent GFA are obtained, respectively. Minor addition based on binary BMGs provides an effective route for developing new BMGs with high GFA.

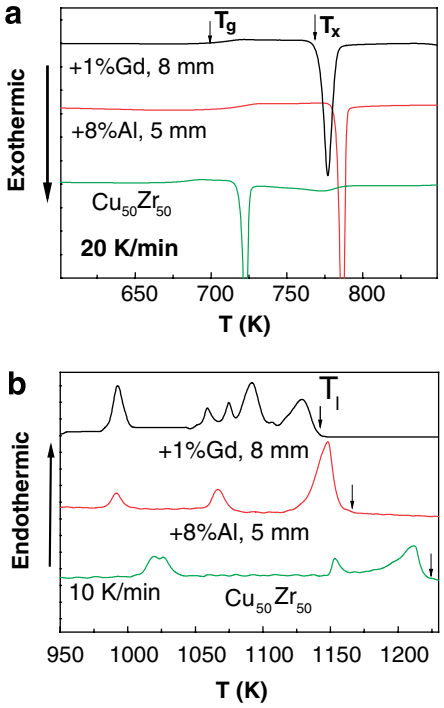

Fig. 29. The DSC (a) and DTA (b) curves of the $Cu_{50}Zr_{50}$, $(Cu_{50}Zr_{50})_{92}Al_8$ and $(Cu_{50}Zr_{50})_{92}Al_7Gd_1$ alloys.

6.2. Unusual GFA induced by minute trace additions

Ce-based BMGs have been developed recently with exceedingly low T_g (below 100 °C) and a large supercooled liquid region ΔT_x [79,105,109,116,117]. These features make the BMG possible to observe the intrinsic viscous behavior of the supercooled liquid near ambient temperature. The 8-mm-diameter BMG bar can be hand-shaped in near-boiling water (see Fig. 30(a)). Such superplasticity (similar to polymeric thermoplastic), which is not expected in crystalline alloys, indicates some potential applications. Fig. 30(b) exhibits its XRD patterns for the as-cast alloys with different minor Co additions. The critical diameter d_c of the alloys as a function of the added Co is illustrated in Fig. 30(c). With minute traces of Co added (0.2%), d_c is dramatically increased from 2 mm to at least 8 mm. The most effective Co addition for improving GFA is below 2%. Such a sensitive change of GFA resulting from minor addition of transition metal contrasts with previous findings that the beneficial addition is usually $\geqslant 1\%$ [21,24,25]. Fe, Si, Nb have similar addition effect on the GFA of the Ce-based BMGs.

It is found that neither ΔT nor T_{rg} reflects the significant changes of the GFA of the alloys induced by minor addition (see the inset of Figs. 30(c) and 31). These alloys with large GFA do not show the expected larger T_{rg}. The T_{rg} and ΔT criteria cannot explain the remarkably large GFA in the Co-microalloying alloys. Neither can the dramatic effect on GFA be explained by the "confusion theory [1]" or by the atomic size factor (Co and component Cu have similar atomic size).

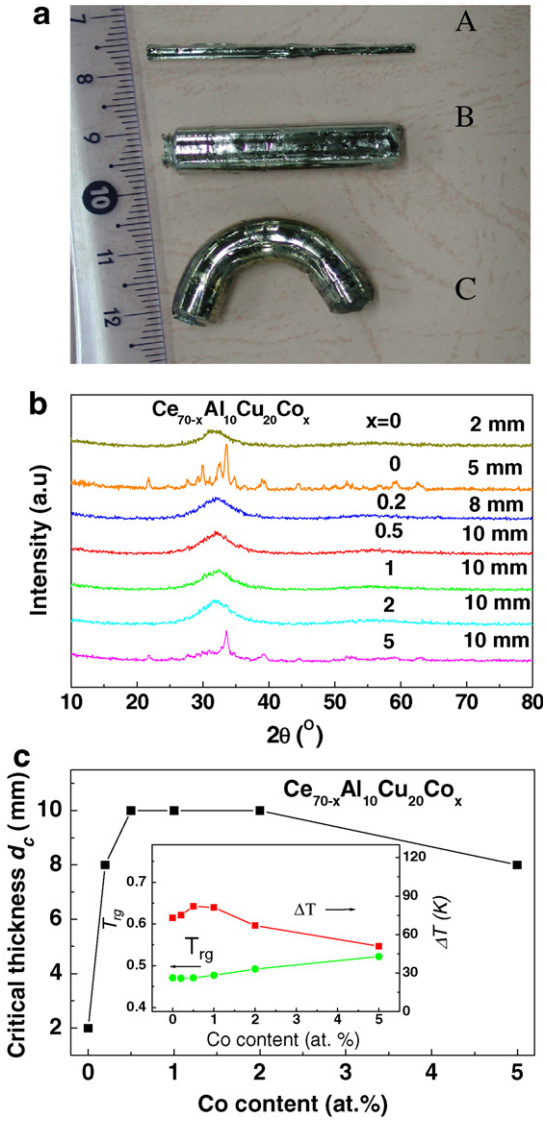

Fig. 30. (a) Picture of the matrix $Ce_{70}Al_{10}Cu_{20}$ BMG bar ($\phi = 2$ mm) (A) and $Ce_{69.8}Al_{10}Cu_{20}Co_{0.2}$ BMG rod ($\phi = 8$ mm) in as-cast state (B) and hand-shaped form in near-boiling water (C). (b) XRD patterns for the matrix alloy and Co microalloyed alloys. (c) The relation between d_c and Co content. A sharp increase of d_c with 0.2% Co microalloying is shown, and the inset shows the changes of T_{rg} and ΔT as functions of Co microalloying content [109].

The changes of density ρ, acoustic velocities and elastic moduli relative to the matrix alloy are contrasted in Fig. 32. All the density, acoustic velocities and elastic moduli show abrupt change for the alloy with 0.2% Co alloying. For example, the relative changes of ρ (0.95%), V_l (2.5%) and K (7.0%) are close to the changes induced by full crystallization in other BMGs (in Zr-based BMG, the crystallization induced relative changes of ρ, V_l and K

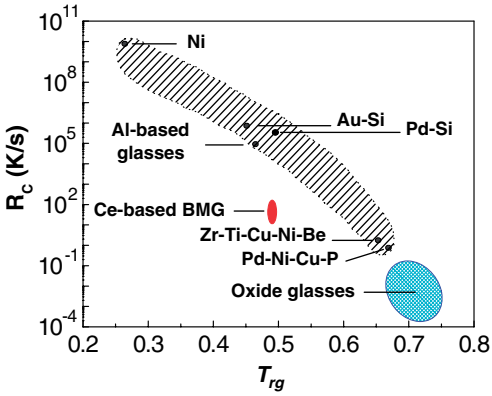

Fig. 31. The relation between T_{rg} and critical cooling rate R_c for various glasses [109].

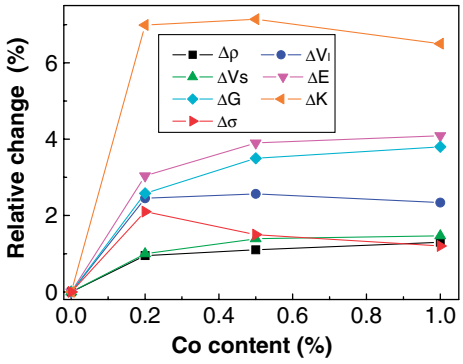

Fig. 32. Relative changes of the density, acoustic velocities and elastic moduli for the Co microalloyed BMGs with respect to the matrix BMG. The ρ, V_l, V_s, E, G, K and σ of the matrix alloy are 6.699 g/cm^3, 2.568 km/s, 1.296 km/s, 29.9 GPa, 11.2 GPa, 29.2 GPa, and 0.329, respectively [109].

are 1.1%, 5.2% and 3.9%, respectively [4]). The results demonstrate that the additions induce sudden structural and property changes in the alloys.

7. Understanding of mechanism of minor addition in glasses formation

We have witnessed encouraging discoveries of centimeter-sized BMGs, such as Cu- [36], Ce- [109], Zr- [1–4], Mg- [40], and Fe-based [23,39] BMGs. The key for the success is attributed to the suitable addition of small amounts into known bulk glass-forming alloys. This success has demonstrated that minor addition represents an effective way to develop novel BMGs. However, due to the complex nature of the multicomponent interactions involved, the alloying effects of the minor additions on glass formation in multicomponent alloys are a complex metallurgic phenomenon, and the underlying mechanism upon the enhancement of GFA by minor addition still remains a puzzling mystery. It thus becomes difficult to identify the optimum amount of a potential element for improving the GFA of a known glass-forming alloy.

To explain the addition effects on a more quantitative level, we focus on studying the addition effect on GFA in simple and typical CuZr alloy. The CuZr meets the larger atomic radius difference criterion (Goldschmidt radii: Cu, 0.128 nm; Zr, 0.161 nm). The size difference leads to copper being an anomalous fast diffuser in zirconium, but zirconium being a slow diffuser in copper [189]. Cu and Zr show a particularly large value of negative heat of mixing ($-23\ \mathrm{kJ\ mol^{-1}}$) [75]. Although binary Cu–Zr appears capable of BMG formation, the system is clearly distinct from a typical multicomponent BMG. Liquids of Cu–Zr have been characterized in terms of Angell's strong/fragile classification [190]. The fragility index m, estimated by heating a Cu–Zr metallic glass is 62 [172] which is significantly higher than the values of 30–40 normally associated with multicomponent BMGs [166,191–195], and identifies the binary liquid as fragile. The GFA and properties of the Cu–Zr alloy is very sensitive to the minor additions [36,37,102,173]. Therefore, CuZr is a model system for studying the mechanism of the minor addition.

The GFA of BMGs is related to the following aspects: (1) liquid structural features and properties, and (2) the stability of competing crystalline phases. Either change the liquid phase (e.g. stability or fragility) or destabilizing the competing crystalline phases can affect the GFA of glass-forming liquids. In the following, we will try to understanding of the role of the minor addition in the formation of the representative BMGs in the aspects of liquid behavior, structure, stability, suppression of the competing crystalline phases and alleviating and purifying the harmful impurities.

7.1. Change the liquid behavior by minor additions

The viscosity (η) with the temperature approaching T_g of glass-forming liquids can be classified according to the concept of "fragility" [190]. The kinetic fragility m, is directly related to the slowing down of the dynamics: it is defined in terms of the shear viscosity as

$$m = \left.\frac{\partial \log \eta(T)}{\partial (T_g/T)}\right|_{T=T_g} \tag{2}$$

If $\eta(T)$ is given by the Vogel–Fulcher–Tammann (VFT) equation:

$$\eta(T) = \eta_0 \exp\left(\frac{D}{T - T_0}\right), \tag{3}$$

where η_0, D, and T_0 are fitting parameters. Then

$$m = \frac{DT_g}{(T_g - T_0)^2 \ln 10} \tag{4}$$

Therefore, m is an index of how fast the viscosity increases while approaching the structural arrest at T_g, the temperature at which the structural relaxation time $\tau \sim 100$ s [190]. The fragility values typically range between $m = 16$ (least value) for "strong" systems and $m = 200$ for "fragile" systems [190]. Recently, it is found that the fragility of a glass-forming liquid is related to the macroscopic properties and GFA of the resulting glass [169,193–200]. The reason might be due to the structure and properties of a glass are essentially the structure and properties of a "frozen" liquid [169].

Since viscosity relaxation and the glass transition measured by calorimetric methods occur on the same time scale, the heating rate, dependent glass transition can be used

as an alternative way to determine the fragility of the glasses [120,116,190–196]. The m for the $Cu_{50}Zr_{50}$, $(Cu_{50}Zr_{50})_{92}Al_8$ and $(Cu_{50}Zr_{50})_{92}Al_7Gd_1$ BMGs are determined to be 62, 43 and 29, respectively. The results show the trend that m decreases with more elements addition. As low as 1% Gd addition makes m sharply decrease to 29. The decrease of m with increasing elements is in good agreement with the trend observed in Zr- [193], Ni-based [194], Al-based [196] and Ce-based alloys [109].

According to the Angell's classification [105], the decrease of m (from 62 to 29) demonstrates that the minor addition has obviously changed the liquid behavior of CuZr into strong family. The small value of m is considered to be one of the empirical rules for designing the BMG formers, whose metastable-equilibrium supercooled liquid is fairly stable [120,191–196]. The results indicate the addition enhance the GFA of the CuZr alloy by strengthening the liquid behavior of the alloys.

In CeCuAl BMGs, one can see in Fig. 33 that a distinct "fragile"–"strong" transition occurs and the fragile matrix liquid is converted to more strong liquid by traces of Co addition [109]. The transition is supported by the jump in apparent heat capacity (ΔC_p) near T_g (see the inset of Fig. 33). A small jump in ΔC_p near T_g suggests a strong resistance to structural degradation in a liquid. For example, the strong liquids like SiO_2 shows a small jump near T_g in ΔC_p while the typical fragile liquids such as AuPbSb alloy and propylene glycol show a sharp peak or large ΔC_p jump [201]. Apparently, the Co bearing alloys exhibit different C_p changes near T_g, and the ΔC_p "jump" is much smaller compared with that of the matrix alloy. When ΔC_p is very small, the configuration entropy $S_c(S_c = \int(\Delta C_p/T)\,dt)$ is almost T-independent, and then according to the Adam–Gibbs equation [202]:

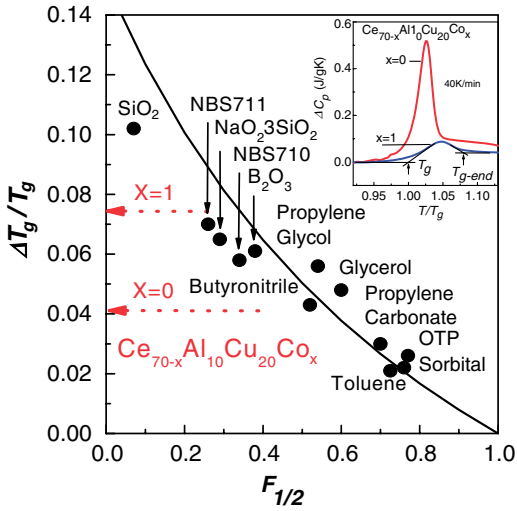

Fig. 33. Relation between $\Delta T_g/T_g$ and $F_{1/2}$. $\Delta T_g/T_g$ has been demonstrated to correlate with the fragility parameter $F_{1/2}$ for inorganic and molecular glasses as a VFT function (the solid line) [199]. We use this correlation to determine the fragility for the present BMGs, and the dashed arrows to the vertical axis show the $\Delta T_g/T_g$ of $Ce_{70-x}Al_{10}Cu_{20}Co_x$ ($x = 0$ and 1) BMGs, which is defined and determined from the T_g-scaled DSC curves at 40 K/min in the inset. The fragility plots (the filled circle) for the inorganic and molecular glasses are taken from Ref. [200].

$$\tau = \tau_0 \exp(A/TS_c), \tag{5}$$

where τ is relaxation time, τ_0 and A are constants. It would predict an Arrhenius temperature dependence of relaxation behavior corresponding to a strong liquid. The correlation of a small value of m with a small jump in ΔC_p upon glass transition conforms that the chemical manipulations of the alloy, by minute traces Co addition, can convert "fragile" liquid into intermediate strong liquid when vitrified at T_g accompanying with dramatically increase of GFA [109]. The superior GFA of the alloys correlates with the strong liquid behavior, which has also been reported in other BMGs [191–196].

7.2. Change the microstructure by minor additions

Experimental and computational evidences indicate that slow-down or glass transition is related to the growth of distinct relaxing domains [203]. The icosahedral clusters in various bulk metallic glass formers have been confirmed by both experiments and simulations [204,205]. New models for metallic glasses were proposed to emphasize the importance of efficient packing of atomic clusters in BMGs [10,204]. The models provide a basis for understanding medium-range order in metallic glasses and allow prediction of new glass-forming alloy compositions. Naturally, the question that arises is how the minor addition can have such markedly effect on the GFA and fragility in the microstructural point of view. Recently, it is found that there exists a correlation between short-range ordering and fragility, e.g. the stronger tendency of short-range ordering in stronger glass formers [206]. It is the degree of short-range ordering in a liquid that controls the fragility. The decrease of m implies that the minor addition induces a strong tendency of short-range ordering in these BMG-forming alloys. The ordering leads to an extra decrease of configuration entropy of the liquid. According to the Adam–Gibbs theory (Eq. (5)) [202], this will result in more viscous and higher density liquid. The high viscosity slows down the crystallization kinetic on cooling, and then enhances the GFA of the alloys.

Ultrasonic measurement, which is powerful for probing subtle structural changes [4], was performed to determine the changes of the sound velocities and elastic constants induced by minor additions in the CuZr- and Ce-based BMGs [37]. It is found that the minor additions induce markedly changes in elastic moduli (e.g. ~5% in shear and Young's moduli) in CuZr-based BMGs [37]. The changes of density, elastic moduli and Debye temperature relative to the matrix CeAlCu alloy are contrasted in Fig. 32 [109]. In the CeAlCu BMGs, the relative density increases 0.95%, 1.1%, and 1.3% for 0.2%, 0.5% and 1% Co microalloyed CeAlCu BMGs, respectively. All the acoustic velocities and elastic moduli show abrupt change for the alloy with 0.2% Co alloying in the Ce-based BMGs. For example, the relative changes of v_l and K are close to the changes induced by fully crystallization in other BMGs (In Zr-based BMG, the crystallization induced relative changes of v_l and K are 5.2% and 3.9%, respectively [4]). A sharp increase of θ_D is also induced by 0.2% Co addition, the distinct increase of θ_D means the acoustic modes in the alloys with Co addition become much stiffer compared with the matrix Co-free alloy. These results demonstrate that significant structural change induced by minor additions. The neutron diffraction and the pair density function analysis also confirm that the additions can change local environments and bonds of the constituents and give rise to topological and chemical ordering [207].

An optimum value of the electronegative difference between the additional element and main components can enhance the GFA, because suitable electronegative difference leads

to the formation of the quasi-covalence (such as the covalent bonding for Al and Co) between the additional element and component [208]. Previous studies show that the BMG-forming alloys showing strong liquid behavior contain a quasi-covalent four-coordinated network [3]. The strong covalent interaction leads to the strong liquid behavior. A covalent bond is much stronger than metallic bonds due to the strong attractive interaction, and thus the covalent bonds are also primarily responsible for a higher degree of atomic packing in the BMGs. The local strong ordering structure with covalent bonds plays the key role in the glass formation. Iron and cobalt were reported to show strong covalent bonding with Al in the metallic glasses [109,209–211]. Thus, Fe and Co microalloying have significant effect on the GFA of the Ce–Al-based alloys [109].

7.3. Stabilize the liquid state of the alloy

It is generally found that minor addition can greatly improve the GFA of alloys via lowering their liquidus temperatures T_l [24,25,36–39,43,44,109,173]. In CuZr alloy, the minor addition makes the T_l decrease from 1219 (for $Cu_{50}Zr_{50}$) to 1139 K (for $(Cu_{50}Zr_{50})_{92}Al_7Gd_1$) (see Fig. 29(b)). Generally, the additional elements have a high tendency of crystalline compound formation with major constituents in a base alloy, which increases its short-range compositional ordering and favors the formation of clusters in the undercooled liquid. It was experimentally confirmed that the local chemical configuration of the clusters in undercooled liquids was extremely different from that of the long-range crystalline ordering [1–4]. In order to form crystalline structure, the atomic pairs in these clusters have to be broken apart upon cooling to form new, stronger chemical bonds with the other constituents. The frustration between the short-range bond ordering and the long-range crystalline ordering actually controls, to some extent, the GFA of the undercooled liquids [1–4]. Therefore, a stronger chemical short-range ordering due to the additions of the proper atoms tends to enhance the liquid phase stability and retards the crystallization process.

On the other hand, the additional small atoms with suitable size (small atoms such as B, Be, and Si) and amount can occupy interstitial spaces among the major constituent atoms, thus increasing the packing density of the liquids [1–4,10,24,25,204]. As such, the liquid phase stability is enhanced. Meantime, additions of small atoms can also enhance the short-range compositional order of glass-forming liquids due to their strong atomic bonding with metallic elements. Consequently, the melting point of the resulting alloy is lowered and the undercooled liquid is stabilized, which are important factors for the BMG formation. Ma et al. [104] present a computational thermodynamic strategy to obtain minor but optimum amount of additional element into a base alloy to improve its GFA, through thermodynamically calculating the maximum liquidus depressions [212] caused by various alloying addition scheme. They have demonstrated the successful use of the approach to significantly improve the GFA of Zr-based as base alloy with the minor addition of Ti [104], and claimed that their computational thermodynamic strategy is robust in locating the bulkiest BMG formers with optimum minor additions.

7.4. Suppress the competing crystalline phases

A suitable addition can suppress the formation of the competing crystalline phases (i.e., primary phases) and favor the glass formation in the alloys. We still use the CuZr system to clarify the issue. The equilibrium phase diagram of Cu–Zr (Fig. 34) [213] shows many

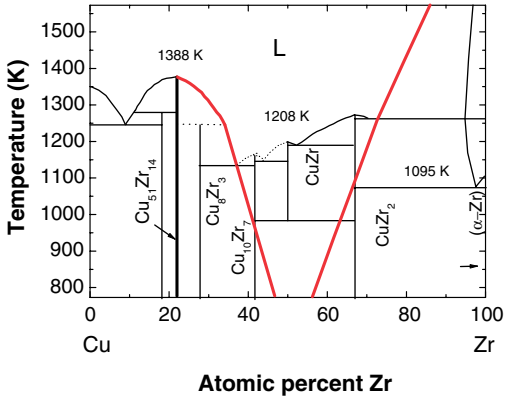

Fig. 34. The equilibrium phase diagram of Cu–Zr. The bold lines indicate the extrapolated liquidus lines for the metastable eutectic of $Cu_{51}Zr_{14}$ and α-Zr. This eutectic applies in the absence of the compounds $CuZr_2$, CuZr, $Cu_{10}Zr_7$ and Cu_8Zr_3 [173].

eutectics depressing the liquidus far below the melting temperatures of the constituent elements, a feature associated with GFA. The main competitor to glass formation in $Cu_{50}Zr_{50}$ on casting at the margin of glass formation is $Cu_{51}Zr_{14}$ (hexagonal, $P6/m$, $a = 1.130$ nm, $c = 0.824$ nm) [173]. Addition of 2 at.% Al changes the primary phase on cooling to Al_2Zr, while addition of 6 at.% Al changes the primary devitrification phase to Al_2Zr_3 [173]. The obviously improved GFA of the glass by addition of aluminum is associated with the suppression of the formation of the competing crystalline phases. This can be interpreted in terms of a deep metastable eutectic between $Cu_{51}Zr_{14}$ and α-Zr [214]. The relevant CuZr metastable phase diagram does not have all the compounds missing, but has $Cu_{51}Zr_{14}$ still present. The heavy lines sketched in Fig. 35 are extrapolations of

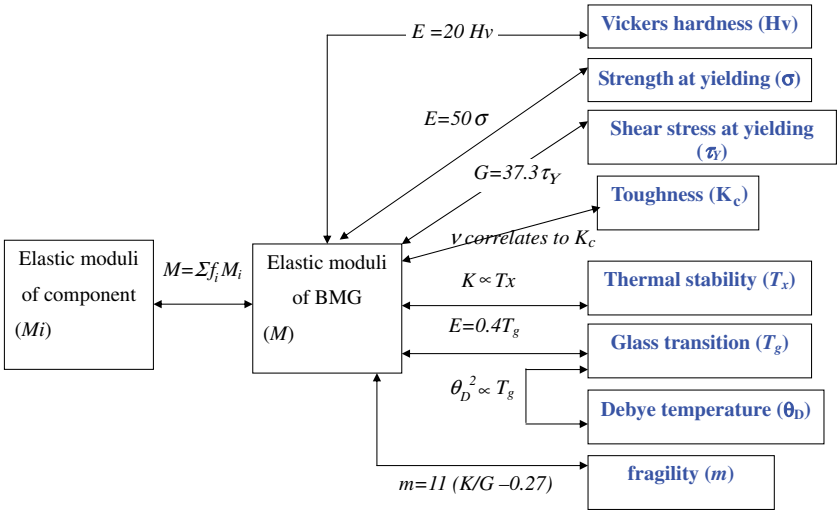

Fig. 35. Schematic diagram to show how the properties of the metallic glasses can be improved or tailored by proper selection of adding component with suitable elastic moduli (M_i).

equilibrium liquidus lines and show the metastable eutectic between $Cu_{51}Zr_{14}$ and α-Zr which appears to be relevant for the good GFA seen at $Cu_{50}Zr_{50}$. Addition inhibits the nucleation and growth of the primary $Cu_{51}Zr_{14}$ phases, and the relevant phase diagram is then a very deep metastable eutectic between the terminal solid-solution phases and thereby promotes glass formation. That is the proper minor additions can adjust alloy composition to a "deeper" eutectic system.

7.5. Alleviating harmful impurity level

The addition such as yttrium can react with the oxygen or the harmful other impurities and form the small particles (e.g. in Zr-based alloy: ZrO). These particles do not trigger the formation of large crystalline phases around them (i.e., do not act as crystallization catalyzing oxides), thus resulting in consuming the oxygen or the other harmful impurities in the alloy [24,25]. From a thermodynamic point of view, the additional element (e.g. yttrium or Gd) has a stronger affinity for the oxygen or other harmful impurities compared with the other elements in the alloy system. For example, the heat of formation of yttrium oxide is 1903.6 kJ/mol, the highest among all oxides of the common base elements (e.g. Fe_2O_3, 820.5 kJ/mol; ZrO, 1102.3 kJ/mol) [75]. The reaction between yttrium and oxygen is thermodynamically favored compared to the reaction between oxygen and the other elements in the system. Therefore, yttrium can effectively neutralize oxygen in the undercooled liquid of Fe-, Zr-, and Mg-based alloys during the melting and casting processes [25,45–51]. The content of oxygen in the remaining liquid was much decreased due to the scavenging effect from yttrium addition.

8. Empirical criteria for applying minor additions

Minor addition technique has shown and will continue playing critical role in enhancing the GFA, improving the manufacturability, tailoring the physical and mechanical properties and thermal stability of BMGs, and exploring novel BMGs. Based on the previous works, the empirical criteria are summarized for enhancing the GFA, for stabilizing the thermal stability, and for formation of composites by minor additions.

8.1. Empirical criteria for improving GFA

From the minor addition technological point of view, based on the experimental results, the GFA of glass-forming alloys can be enhanced by the following considerations:

(1) The selected adding elements have large negative heat of mixing with the main components of the alloy. The high tendency of compound formation of the additional elements can suppress the competitive crystalline phases during glass formation.
(2) The selected elements have high affinity with oxygen and other harmful impurities to glass formation, and the formed compounds should have markedly different structures from that of the competitive crystalline phase. Then, the minor addition can minimize oxygen impurity and purify the glass-forming alloy to form the innocuous oxides.
(3) The selected elements can depress the melting temperature of the glass-forming alloy, or adjust the composition close to the deep eutectic.

(4) The selected adding elements have large atomic mismatch with the major constituents of the glass-forming alloy.
(5) An optimum value of the electronegative difference between the minor adding element and main components can enhance the GFA, because suitable electronegative difference leads to the formation of the quasi-covalence between the additional element and component.
(6) The selected elements can make the glass-forming liquid stronger or decrease the value of the fragility, m.
(7) The selected adding elements can change the microstructural feature, and favor the formation of the local strong ordering structure, and then favor the formation of a higher degree of atomic packing or an increased complexity in the glass-forming liquid.
(8) The selected adding elements have large solubility in the glass-forming alloy, which can make the homogeneously microalloying process.

8.2. Empirical criteria for enhancing the properties

8.2.1. Stabilizing the thermal stability

To enhance the thermal stability of the BMGs without impairing the GFA of glass-forming alloys, the minor addition can fellow the following considerations:

(1) Selecting the small atoms that can increase the density of the randomly packed structure of the liquids.
(2) Adding the atoms that can lower the melting point and then stabilize the liquid phase.
(3) Selecting the atom that can suppress the nucleation and crystal growth processes of the competing crystalline phases.
(4) Select the atoms that can scavenge the oxygen and other harmful impurities out of the alloy liquid to form innocuous oxides.

It should be note that GFA and thermal stability of metallic glasses are different properties, and minor alloying additions can show contrasting results in a given system.

8.2.2. Enhancing the mechanical and physical properties

The experimental data reveal clearly correlations between linear elastic constants and mechanical properties, plastic yielding of the glass, thermal stability, and rheological properties of the glass-forming liquid [8,91,166–171]. Meanwhile, the elastic moduli (M) of metallic glasses scale with those of their elemental components (see Fig. 35). Therefore, the controlled elastic moduli of the alloy can be used to control of the properties of the glass. This means the properties of the glass can be improved or tailored by proper selection of adding component with suitable elastic moduli (M_i) [8,91,166–170].

8.3. Empirical criteria for formation of BMG-based composites by minor additions

The BMG-based composites can be formed by minor addition through the following considerations:

(1) The adding elements have large negative heat of mixing with one of the main components of the alloy, and the formed compounds will not trigger the crystallization of the liquid and significantly degrade the GFA of the alloy.
(2) The addition-induced compounds should be of unique properties wanted, and then the properties of the composites can be improved.
(3) The adding materials can induce controllable crystallization, which can induce significant nucleation but the formed nuclei have low growth rate, and then the controllable crystallization (e.g. nanocrystallization) can occur in the alloy.
(4) The large solubility of the addition materials in the matrix alloy is necessary for homogenous distribution of the formed second phase in the BMG matrix.

9. Summary

The comprehensive review of the recent developments in minor addition or microalloying technique, presented in these pages has shown that this technique, which has been widely used in other metallurgical fields, shows effective and important roles in the bulk metallic glass formation, BMG-based composites formation, crystallization control, thermal stability, and mechanical and physical properties improvements of BMGs. We have witnessed encouraging discoveries of centimeter-sized BMGs, BMG-based composites with much improved mechanical and physical properties, and unique BMGs with excellent mechanical properties. The key for these successes might be attributed to the suitable addition of small amounts into known bulk glass-forming alloys. The successes have demonstrated that the minor addition approach represents a feasible way to develop and design novel BMGs. It is believed that more novel BMG materials with excellent GFA and unique mechanical and physical properties will be continually developed by means of this method.

Up to now, almost all the approaches to bulk fabrication of metallic glasses were mostly empirical in nature. The main proposed empirical rules for bulk metallic glass formation are: (1) multicomponent systems consisting of more than three elements; (2) significant difference in atomic sizes with the size ratios above about 12% among the three main constituent elements; and (3) negative heats of mixing among the three main constituent elements; (4) "confusion principle"; (5) the alloy with a composition close to deep eutectic. It is found that the alloys satisfying these empirical rules have special atomic configurations in the liquid state which is significantly different from those of the corresponding crystalline phases, and the atomic configurations favor the glass formation. The beneficial effects of minor addition on the glass-forming ability, and the thermal stability satisfy these empirical rules, and can be understood in terms of thermodynamics, kinetics as well as the microstructural aspects. In microstructure, the minor addition favors the formation of the unique atomic dense configurations with small free volumes, strong liquid behavior, and high viscosity which are significantly different from those for conventional metallic glasses. Thermodynamically, the minor addition makes the melts energetically closer to the crystalline state than other metallic melts due to their high packing density in conjunction with a tendency to develop short-range order. Kinetically, the minor addition makes the melts more viscous which leads to slow crystallization kinetics. Minor addition can also purify the melt and interfere the nucleation and growth of the competitive crystalline phases of the glass. The empirical criteria, or the guidelines for the applying minor addition technique in BMG field are outlined.

It should be noted that the effect of minor addition on the glass-forming ability is complicated and bears many of the fundamental features of glass formation and features. The lack of a fundamental theory of glass formation is directly related to the lack of a fundamental theory about the role of the minor addition in glass formation. It is hoped that the present paper at least shows the importance of the minor addition technique to the problem of synthesizing and enhancing the bulk metallic glasses.

With the development of the BMG field, significant amounts of data have been collected on the mechanical, elastic, physical and other properties of various BMGs. Recently, extensive attempts have been made to correlate these properties including the fragility of glass-forming liquid of these glasses. Some plausible correlations have been established. These established correlations, at least the correlations associated with elastic moduli, provide useful guidelines for controlling or enhancing the properties of the BMGs using minor addition by selection of components with optimized elastic moduli.

Minor addition is also feasible for the formation of BMG based composites with unique or improved properties, and the proper adding materials can induce controllable crystallization, which can induce significant nucleation but the formed nuclei are difficult to grow. The formed crystalline compounds induced by addition will not trigger the crystallization of the liquid and significantly degrade the GFA of the alloy. The large solubility of the addition materials is necessary for homogenous distribution of the formed second phase in the BMG matrix.

Minor addition is useful for improve the manufacturability of BMGs by purifying the alloy, scavenging the oxygen and other harmful impurities from the undercooled liquid.

The open issues for the minor addition are: (1) the lack of the fundamental theory about the mechanism of the minor addition in glass formation and properties tailoring; (2) no feasible criteria or strategy to locate the optimum effect for improving and enhancing the formation and properties of BMG with optimum minor additions. A lot still remains to be done for a clear image to appear.

Acknowledgements

The author is indebted to Prof. A.L. Greer, Prof. K. Samwer, Prof. C.T. Liu, Prof. T.G. Nieh, Prof. Y. Wu, Prof. J. Eckert, Prof. J.J. Lewandowski, Prof. G. Johari for valuable discussions and support. The experimental assistances and discussions from Prof. M.X. Pan, Prof. R.J. Wang, D.Q. Zhao, Prof. H.Y. Bai, Prof. Y. Zhang, Prof. B.C. Wei, Dr. P. Wen, Dr. L. Xia, Dr. X.K. Xi, Dr. Y.X. Wei, Dr. Y.H. Zhao, B. Zhang, S. Li, M.B. Tang, Y. Hu, Z.F. Zhao, Y.T. Wang, Q. Luo, B. Yu and Yong Li, and the financial support of the National Natural Science Foundation of China (Grant Nr: 50321101) are appreciated.

References

[1] Greer AL. Science 1995;267:1947.
[2] Johnson WL. MRS Bull 1999;24:42.
[3] Inoue A. Acta Mater 2000;48:279.
[4] Wang WH, Dong C, Shek CH. Mater Sci Eng R 2004;44:45.
[5] Ashby MF, Greer AL. Scripta Mater 2006;54:321.
[6] Kim JJ, Choi Y, Suresh S, Argon AS. Science 2002;295:654.
[7] Tang XP, Geyer U, Busch R, Johnson WL, Wu Y. Nature 1999;402:160.

[8] Schroers J, Johnson WL. Phys Rev Lett 2004;93:255506.
[9] Miracle DB. Nature Mater 2004;3:697.
[10] Sheng HW, Luo WK, Alamgir FM, Bai JM, Ma E. Nature 2006;439:419.
[11] http://www.liquidmetal.com.
[12] Macfarlane A. Science 2004;305:1407.
[13] Clement W, Willens RH, Duwez P. Nature 1960;187:869.
[14] Daveis HA. In: Luborsky FE, editor. Amorphous metallic alloys. London: Butterworts; 1983.
[15] Kavesh S. In: Gillman JJ, Leamy HL, editors. Metallic glasses. Metals Park, OH: ASM International; 1978 [Chapter 2].
[16] Takayama S. J Mater Sci 1976;11:164.
[17] Turnbull D. Prog Solid State Phys 1956;3:225.
[18] Turnbull D, Fisher JC. J Chem Phys 1949;17:71.
[19] Turnbull D. Contemp Phys 1969;10:437.
[20] Kui WH, Greer AL, Turnbull D. Appl Phys Lett 1984;45:615.
[21] Inoue A, Zhang T, Masumoto T. Mater Trans JIM 1989;30:965.
[22] Greer AL. Nature 1993;366:303.
[23] Lu ZP, Liu CT. Phys Rev Lett 2003;91:115505.
[24] Wang WH, Bian Z, Wen P, Pan MX, Zhao DQ. Intermetallic 2002;10:1249.
[25] Lu ZP, Liu CT. J Mater Sci 2004;39:3965;
Liu CT, Lu ZP. Intermetallics 2005;13:415.
[26] Liu CT, White CL, Horton JA. Acta Metall 1985;33:213.
[27] Nishizawa T. Mater Trans 2001;42:2027.
[28] Greer AL. Phil Trans Royal Soc Lond A 2003;361:479;
Guiner A. Nature 1938;142:569.
[29] Pattersen K, Bakke P, Albright D. Magnesium die casting alloy design. Warrendale, PA: TMS; 2002 [p. 241–6].
[30] Inoue A, Nishiyama N, Kimura H. Mater Trans JIM 1997;38:179.
[31] Louzguine DV, Inoue A. J Mater Res 1999;14:4426.
[32] Li C, Saida J, Matsushida M, Inoue A. Script Mater 2000;42:923.
[33] Liu W, Johnson WL. J Mater Res 1996;11:2388.
[34] Kang HG, Park ES, Kim WT, Kim DH, Cho HK. Mater Trans JIM 2000;41:846.
[35] Inoue A, Zhang T, Koshiba H. J Appl Phys 1998;83:6326.
[36] Xu D, Duan G, Johnson WL. Phys Rev Lett 2004;92:245504.
[37] Yu P, Bai HY, Wang WH. J Mater Res 2006;21:1674.
[38] Lu ZP, Liu CT, Thompson JR, Porter WD. Phys Rev Lett 2004;92:245503.
[39] Shen J, Chen QJ, Sun JF, Fan HB, Wang G. Appl Phys Lett 2005;86:151907.
[40] Ma H, Shi LL, Xu J, Li Y, Ma E. Appl Phys Lett 2005;87:181915.
[41] Gebert A, Eckert J, Schultz L. Acta Mater 1998;46:5475.
[42] Zhang Y, Pan MX, Wang RJ, Wang WH. Mater Trans JIM 2000;41:1410.
[43] Wang WH, Wei Q, Bai HY. Appl Phys Lett 1997;71:58.
[44] Wang WH, Wang RJ, Eckert J. Mater Trans JIM 2001;42:587.
[45] Hu Y, Pan MX, Liu L, Wang WH. Mater Lett 2003;57:2698.
[46] Luo CY, Pan MX, Xi XK, Zhao DQ, Wang WH. J Non-Cryst Solids 2006;352:185.
[47] Zhao YH, Luo CY, Pan MX, Wang WH. Intermetallics 2006;14:1107.
[48] Men H, Kim DH. J Mater Res 2003;18:1502.
[49] Xi XK, Zhao DQ, Pan MX, Wang WH. J Non-Cryst Solids 2004;344:105.
[50] Wei YX, Xi XK, Zhao DQ, Pan MX, Wang WH. Mater Lett 2005;59:945.
[51] Xi XK, Zhao DQ, Pan MX, Wang WH. J Non-Cryst Solids 2004;344:189.
[52] Choi-Yim H, Busch R, Koster U, Johnson WL. Acta Mater 1999;47:2455.
[53] He G, Eckert J, Loeser W, Schultz L. Nature Mater 2003;2:33;
Kato H, Inoue A. Mater Trans JIM 1997;38:793.
[54] Wang WH, Bai HY. Mater Lett 2000;43:59.
[55] Wang WH, Bai HY. J Appl Phys 1998;84:5961.
[56] Bian Z, Wang RJ, Pan MX, Zhao DQ, Wang WH. Adv Mater 2003;15:616.
[57] Conner RD, Choi-Yim H, Johnson WL. J Mater Res 1999;14:3292.
[58] Hays CC, Kim CP, Johnson WL. Phys Rev Lett 2000;84:2901.

[59] Kim CP, Bush R, Masuhr A, Johnson WL. Appl Phys Lett 2001;79:1456.
[60] Brothers H, Dunand DC. Adv Mater 2005;17:484.
[61] Shek CH, Sun YF, Wei BC. J Alloys Comp 2005;403:239.
[62] Wang WH, Pan MX, Zhao DQ, Hu Y, Bai HY. J Phys: Condens Matter 2004;16:3719.
[63] Zhang Z, Wang WH. J Mater Res 2005;20:314.
[64] He G, Eckert J, Loser W. Acta Mater 2003;51:1621.
[65] Wang YT, Pan MX, Zhao DQ, Han BS, Wang WH. J Non-Cryst Solids 2006;352:444.
[66] Das J, Tang MB, Kim KB, Theissmann R, Baier F, Wang WH, et al. Phys Rev Lett 2005;94:205501.
[67] Lee SW, Huh MY, Fleury E, Lee JC. Acta Mater 2006;54:349.
[68] Xing LQ, Ramesh KT, Hufnagel TC. Phys Rev B 2001;64:180201.
[69] Wang G, Wang WH. In press.
[70] Lin XH, Johnson WL. J Appl Phys 1995;78:6514.
[71] Ma C, Soejima H, Amiya K, Nishiyama N, Inoue A. Mater Trans 2004;45:3223.
[72] Shen B, Inoue A. J Mater Res 2004;21:4911.
[73] Ponnambalam V, Poon SJ, Shiflet GJ. J Mater Res 2004;19:1320.
[74] Yao B, Si L, Tan T, Zhang Y, Li Y. J Non-Cryt Solids 2003;323:43.
[75] Boer FR, Boom R, Matterns WCM, Miedema AR, Niessen AK. Cohesion in metals. Amsterdam: North-Holland; 1988.
[76] Choi-Yim H, Busch R, Johnson WL. J Appl Phys 1998;83:7993.
[77] Yi S, Lee JK, Kim WT, Kim DH. J Non-Cryst Solids 2001;291:132.
[78] Inoue A, Murakami A, Zhang T, Takeuchi A. Mater Trans JIM 1997;38:189.
[79] Zhang B, Zhao DQ, Pan MX, Wang WH. Acta Mater 2006;54:3025.
[80] Park ES, Lim HK, Kim WT, Kim DH. J Non-Cryst Solids 2002;298:15.
[81] Liu CT, Chisholm MF, Miller MK. Intermetallics 2002;10:1105.
[82] Ozaki K, Kobayashi K, Nishio T. Mater Trans JIM 1998;39:499.
[83] Choi-Yim H, Xu D, Johnson WL. Appl Phys Lett 2003;82:1030.
[84] Inoue A, Wang XM. Acta Mater 2000;48:1383.
[85] Inoue A, Negishi T, Kimura H, Aoki T. Mater Trans JIM 1997;38:185.
[86] Ponnambalam V, Poon SJ, Shiflet GJ. Appl Phys Lett 2003;83:1132.
[87] Lu ZP, Liu CT, Porter WD. Appl Phys Lett 2003;83:2581.
[88] Inoue A, Shen BL, Koshiba H, Kato H, Yavari AR. Nature Mater 2003;2:661.
[89] Hess PA, Poon SJ, Shiflet GJ, Dauskardt RH. J Mater Res 2005;20:783.
[90] Xi XK, Zhao DQ, Pan MX, Wang WH, Wu Y, Lewandowski JJ. Phys Rev Lett 2005;94:125510.
[91] Lewandowski JJ, Wang WH, Greer AL. Philos Mag Lett 2005;85:77.
[92] Itoi T, Inoue A. Mater Trans JIM 2000;41:1256.
[93] Zhao DQ, Zhang Y, Pan MX, Wang WH. Mater Trans JIM 2000;41:1427.
[94] Zhang T, Yamamoto T, Inoue A. Mater Trans 2002;43:3222.
[95] Fan GJ, Echert J, Schultz L. Appl Phys Lett 1999;75:2984.
[96] Men H, Hu ZQ, Xu J. Scripta Mater 2002;46:699.
[97] Qin CL, Inoue A. Mater Trans 2003;44:1042.
[98] Inoue A, Shibata T, Zhang T. Mater Trans JIM 1995;36:1420.
[99] Mitrovic N, Roth S, Eckert J. Appl Phys Lett 2001;78:2145.
[100] Inoue A, Shen B. Mater Trans 2002;43:1230.
[101] Men H, Pang S, Inoue A, Zhang T. Mater Trans 2005;46:2218.
[102] Yu P, Bai H. J Non-Cryst Solids 2005;351:1328.
[103] Zhang Y, Zhao DQ, Wang RJ, Dong YD, Wang WH. Script Mater 2001;44:1107.
[104] Ma D, Cao H, Ding L, Chang YA, Hsieh KC, Pan Y. Appl Phys Lett 2005;87:171914.
[105] Zhang B, Zhao DQ, Pan MX, Wang WH, Greer AL. Phys Rev Lett 2005;94:205502.
[106] Guo F, Wang HJ, Poon SJ, Shiflet GJ. Appl Phys Lett 2005;86:091907.
[107] Xia J, Qiang J, Wang Y, Wang Q, Dong C. Appl Phys Lett 2006;88:101907.
[108] Shen BL, Akiba M, Inoue A. Phys Rev B 2006;73:104204.
[109] Zhang B, Wang WH. Phys Rev B 2006;73:092201.
[110] Xing DW. Nonferr Metal Soc 2003;13:68.
[111] Zheng ZJ, Li HY. Rare earth functional materials. Beijing: Chemical Industry Press; 2003.
[112] Li S, Wang RJ, Pan MX, Zhao DQ, Wang WH. Sci Tech Adv Mater 2005;6:823.
[113] Li S, Wang WH. J Non-Cryst Solids 2005;351:2568.

[114] Wei BC, Wang WH, Pan MX, Han BS. Phys Rev B 2001;64:012406.
[115] Guo F, Poon SJ, Shiflet GJ. Appl Phys Lett 2003;83:2575.
[116] Zhang B, Wang WH. Phys Rev B 2004;70:224208.
[117] Zhang B, Pan MX, Zhao DQ, Wang WH. Appl Phys Lett 2004;85:61.
[118] Xi XK, Li S, Wang RJ, Zhao DQ, Pan MX, Wang WH. J Mater Res 2005;20:2243.
[119] Zhang Y, Tan H, Li Y. Mater Sci Eng A 2004;375:436.
[120] Zhao ZF, Pan MX, Zhao DQ, Wang WH. Appl Phys Lett 2003;82:4699.
[121] Zhang Y, Pan MX, Zhao DQ, Wang WH. Formation of Zr-based bulk metallic glasses from the low purity materials by yttrium addition. US Patent Nr. US6682611B2.
[122] Xi XK, Zhao DQ, Pan MX, Wang WH. Intermetallics 2005;13:638.
[123] Zhao YH, Pan MX, Wang WH, Eckert J. J Phys D: Appl Phys 2005;38:2162.
[124] Kundig AA, Lepori D, Perry AJ, Rossmann S, Blatter SA, Dommann A, et al. Mater Trans 2002;43:3206.
[125] Chen J, Zhang Y, He JP, Yao KF, Wei BC, Chen GL. Scripta Mater 2006;54:1351.
[126] Men H, Pang SJ, Zhang T. J Mater Res 2006;21:958.
[127] Eckert J, Mattern M, Zinkevitch M, Seidel M. Mater Trans JIM 1998;39:623.
[128] Murty BS, Ping DH, Hono K, Inoue A. Acta Mater 2000;48:3985.
[129] Altounian Z, Batalla E, Strom-Olsen JO. J Appl Phys 1986;61:149.
[130] Conner RD, Maire RE, Johnson WL. Mater Sci Eng A 2006;419:148.
[131] Huett VT, Zander D, Jastrow L, Majzoub EH, Kelton KF, Koster U. J Alloys Comp 2004;379:16.
[132] Kokanovic I, Tonejc A. J Alloys Comp 2004;377:141.
[133] Sordelet DJ, Yang XY, Rozhkova EA, Kramer MJ. Appl Phys Lett 2003;83:69.
[134] Chen MW, Inoue A, Sakurai T, Ping DH, Hono K. Appl Phys Lett 1999;74:812.
[135] Kubler A, Eckert J, Gebert A, Schultz L. J Appl Phys 1998;83:3438.
[136] Jayalakshmi S, Kim KB, Fleury E. J Alloys Comp 2006;417:195.
[137] Dong W, Zhang HF, Sun W, Hu Z. Mater Trans 2006;47:1249;
Liu WY, Zhang HF, Hu ZQ. Mater Sci Forum 2005;488–489:211.
[138] Jiang F, Wang ZJ, Sun J. Scripta Mater 2005;53:482.
[139] Spaepen F. Acta Mater 1977;25:407.
[140] Lewandowski JJ, Greer AL. Nature Mater 2006;5:15.
[141] Schuh CA, Lund AC, Nieh TG. Acta Mater 2004;52:5879.
[142] Fan C, Li H, Kecskes LJ, Tao K, Choo H, Liaw PK, Liu CT. Phys Rev Lett 2006;96:145506.
[143] Kühn U, Eckert J, Mattern N, Schultz L. Appl Phys Lett 2002;80:2478.
[144] Wang WH, Wang RJ, Zhao DQ, Pan MX. Appl Phys Lett 1999;74:1803.
[145] Ma H, Xu J, Ma E. Appl Phys Lett 2003;83:2793.
[146] Ibrahim IA, Mohamed FA, Lavernia EJ. J Mater Sci 1991;26:1137.
[147] Bae DH, Lee MH, Kim DH, Sordelet DJ. Appl Phys Lett 2003;83:2312.
[148] Inoue A, Zhang T, Saida J, Matsushita M. Mater Trans JIM 2000;41:1511.
[149] Xing LQ, Eckert J, Schultz L. Nanostruct Mater 1999;12:503.
[150] Chen MW, Zhang T, Inoue A, Sakurai T. Appl Phys Lett 1999;75:1697.
[151] Inoue A, Zhang W, Tsuruiy T, Yavari AR, Greer AL. Philos Mag Lett 2005;85:221.
[152] Trancy MM, Ebbesen TW, Gibson JM. Nature (London) 1996;381:678.
[153] Schroers J, Veazey C, Johnson WL. Appl Phys Lett 2003;82:370.
[154] Brothers AH, Dunaud DC. Appl Phys Lett 2004;84:1108.
[155] Wada T, Inoue A. Mater Trans 2003;44:2228.
[156] Inoue A, Zhang T, Chen MW, Sakurai T, Saida J. Appl Phys Lett 2000;76:967.
[157] Xing LQ, Eckert J, Löser W, Schultz L. Appl Phys Lett 1999;74:664.
[158] Scudino S, Kühn U, Schultz L, Lüders K, Eckert J. J Mater Sci 2004;39:5483.
[159] Saida J, Matsushita M, Inoue A. Mater Trans JIM 2000;41:543.
[160] González J, González JM. In: Nalwa HS, editor. Encyclopedia of nanoscience and nanotechnology, vol. 10. Baltimore: American Scientific; 2004. p. 1.
[161] Iturriza N, García C, Fernández L, Val del JJ, González J, Blanco JM, et al. J Appl Phys 2006;99:08F104.
[162] Willard MA, Laughlin DE, McHenry ME, Thoma D, Sickafus K, Cross JO, et al. J Appl Phys 1998;84:6773.
[163] Tate BJ, Todd I, Davies HA, Gibbs MRJ, Mayor RV. J Appl Phys 1998;83:6335.
[164] Agudo P, Vázquez M. J Appl Phys 2005;97:023901.
[165] Shen B, Inoue A. Mater Trans 2002;43:1235.

[166] Wang WH. J Appl Phys 2006;99:093506.
[167] Wei YX, Zhang B, Pan MX, Zhao DQ, Wang WH. Scripa Mater 2006;54:599.
[168] Egami T. Mater Sci Eng A 1997;226:261.
[169] Novikov VN, Sokolov AP. Nature 2004;432:961.
[170] Johnson WL, Samwer K. Phys Rev Lett 2005;95:195501.
[171] Wang WH. J Non-Cryst Solids 2005;351:1481.
[172] Tang MB, Zhao DQ, Pan MX, Wang WH. Chinese Phys Lett 2004;21:901.
[173] Wang WH, Lewendowski JJ, Greer AL. J Mater Res 2005;20:2307.
[174] Yokoyama Y, Fukaura K, Inoue A. Mater Trans 2004;45:1672.
[175] Gu XJ, McDermott AG, Poon SJ, Shiflet GJ. Appl Phys Lett 2006;88:211905.
[176] Franco V, Borrego JM, Conde A, Roth S. Appl Phys Lett 2006;88:132509.
[177] Qiu CL, Liu L, Sun M. J Biomed Mater Res 2005;75A:950.
[178] Liu L, Qiu CL, Zou H. J Alloys Comp 2005;399:144.
[179] Nishiyama N, Inoue A, Jiang JZ. Appl Phys Lett 2001;78:1985.
[180] Wang WH, Wang RJ, Yao YS. Phys Rev B 2000;62:11292.
[181] Leonhardt M, Loser W, Lindenkreuz H-G. Acta Mater 1999;47:2961.
[182] Xia L, Li WH, Wei BC, Dong YD. J Appl Phys 2006;99:026103.
[183] Guo FQ, Poon SJ, Shiflet GJ. Appl Phys Lett 2004;84:37.
[184] Yao KF, Fang R. Chin Phys Lett 2005;22:1481.
[185] Kolesnikov AI, Howells WS, Harkunov AI. Phys Rev B 1999;60:12681.
[186] Wang D, Li Y, Sun BB, Sui ML, Lu K, Ma E. Appl Phys Lett 2004;84:4029.
[187] Xu D, Lohwongwatana B, Duan G, Johnson WL, Garland C. Acta Mater 2004;52:2621.
[188] Inoue A, Zhang W. Mater Trans 2004;45:584.
[189] Le Claire AD. J Nucl Mater 1978;69–70:70.
[190] Angell CA. Science 1995;267:1924.
[191] Perera DN. J Phys: Condens Matter 1999;11:3807.
[192] Bruning R, Samwer K. Phys Rev B 1992;46:11318.
[193] Busch R, Bakke E, Johnson WL. Acta Mater 1998;46:4725.
[194] Shadowspeaker L, Busch R. Appl Phys Lett 2004;85:2508.
[195] Borrego JM, Conde A, Roth S, Eckert J. J Appl Phys 2002;92:2073.
[196] Louzguine DV, Sobu S, Inoue A. Appl Phys Lett 2004;85:3758.
[197] Angell CA. J Non-Cryst Solids 1985;73:1.
[198] Sokolov AP, Rossler E, Kisliuk A, Quitmann D. Phys Rev Lett 1993;71:2062.
[199] Scopigno T, Ruocco G, Sette F, Monako G. Science 2003;302:849.
[200] Ito K, Moynihan CT, Angell CA. Nature (London) 1999;398:492.
[201] Fecht HJ. Mater Trans JIM 1995;36:777.
[202] Adam G, Gibbs JH. J Chem Phys 1965;43:139.
[203] Debenedetti PG, Stillinger FH. Nature 2001;410:259.
[204] Miracle D. Nature Mater 2004;3:697.
[205] Li J, Gu X, Hufnagel TC. Microsc Microanal 2003;9:509.
[206] Tanaka H. Phys Rev Lett 2003;90:055701.
[207] Ahn K, Louca D, Poon SJ, Shiflet GJ. Phys Rev B 2004;70:224103.
[208] Louzguine DV, Inoue A. Appl Phys Lett 2001;79:3410.
[209] Hsieh HY, Toby BH, Egami T, He Y, Poon SJ, Shiflet GJ. J Mater Res 1990;5:2807.
[210] Mansour AN, Wong CP, Brizzolara RA. Phys Rev B 1994;50:12401.
[211] Mizuno M, Araki H, Shirai Y. Phys Rev B 2003;68:144103.
[212] Chang YA, Chen S, Zhang F, Yan X, Xie F, Schmid-Fetzer R, et al. Prog Mater Sci 2004;49:313.
[213] Zeng KJ, Hamalainen M, Lukas HL. J Phase Equilibria 1994;15:577.
[214] Highmore RJ, Greer AL. Nature 1989;339:363.